2020-24-0009 Published 27 Sep 2020

A Simulation Study Assessing the Viability of Shifting the Location of Peak In-Cylinder Pressure in Motored Experiments

Gilbert Sammut Jaguar & Land Rover

Emiliano Pipitone University of Palermo

Carl Caruana and Mario Farrugia University of Malta

Citation: Sammut, G., Pipitone, E., Caruana, C., and Farrugia, M., "A Simulation Study Assessing the Viability of Shifting the Location of Peak In-Cylinder Pressure in Motored Experiments," *SAE Int. J. Advances & Curr. Prac. in Mobility* 3(2):894-913, 2021, doi:10.4271/2020-24-0009.

This article was presented at the Conference on Sustainable Mobility, Catania, Italy, Oct. 4-7, 2020.

Abstract

Hybrid powertrains utilize an engine to benefit from the power density of the liquid fuel to extend the range of the vehicle. On the other hand, the electric machine is used for; transient operation, for very low loads and where legislation prohibits any gaseous and particulate emissions. Consequently, the operating points of an engine nowadays shifted from its conventional, broad range of speed and load to a narrower operating range of high thermal efficiency. This requires a departure from conventional engine architecture, meaning that analytical models used to predict the behavior of the engines early in the design cycle are no longer always applicable. Friction models are an example of sub-models which struggle with previously unexplored engine architectures. The "pressurized motored" method has proven to be a simple experimental setup which allows a robust FMEP determination against which engine friction simulation can be fine-tuned. This is due to the elimination of the experimental variability introduced by combustion, whilst retaining the fired-like load on the cranktrain, as reported in SAE 2018-01-0121. It employs a "shunt pipe" recirculating air from the exhaust back into the intake, therefore requiring very little air supply demands. The temperature of the bulk gas was also maintained similar to that of a fired engine with the use of Argon as the working gas, reported in SAE 2019-01-0930. Mixtures of Argon-to-air were also used to investigate the effect of temperature on FMEP, published in SAE 2019-24-0141 and SAE 2020-01-1063. This leaves one pending criticism of the pressurized motoring method - that of having a relatively fixed location of peak pressure (≈1DegCA BTDC), when compared to a fired engine, which is around 10DegCA for CI and 20DegCA for SI. In this publication, a simulation investigation is performed to assess the viability and extent of an experimental modification to the pressurized motoring method, involving the use of small fuel injections to shift the location of peak pressure in the aim of replicating better the fired engine, whilst retaining the benefits of a motored setup.

Introduction

Recent legislations on internal combustion engine emissions have put great challenges on the automotive industry. Engine designers are forced to explore new routes in their design processes, like for example resorting to hybrid technology. In this deviation away from the conventional operation of the internal combustion engine, a shift in the operating points of the engine is typically done to ensure the engine is used only at conditions in which the electric drive is not capable of meeting the demand, and sometimes operating in narrow ranges where the engine has high thermal efficiencies.

Models which are often used in the engine design stage are, in their majority, derived from conventional engines running at traditional operating conditions. When faced with new engine designs, these models struggle to give accurate prediction, as their foundations are too detached from the present requirements. The models used for mechanical friction are among these. Proposing any changes or new models altogether, requires the support of robust and reliable experimental data on modern representative engines.

Obtaining reliable and robust mechanical friction experimental data have proved challenging over the years [1, 2, 3]. Difficulties which are usually met in this endeavor include the requirement of fully-equipped experimental setups which are able to conduct measurements at very high precision and very minimal variance. This may be obtained through an accurate conditioning of the external influences, in combination with an appropriate method of FMEP determination.

The FMEP quantity is usually relatively small in magnitude, when compared to the fired IMEP and the fired BMEP. This creates a challenge to determine with good accuracy and fidelity. Richardson [4] and Mauke [3] give an extensive review of several methods stating their strong points and also their

shortcomings. Some of the popular FMEP determination experimental methods include the fired indicating method, the teardown test, Morse test, motoring tests and the instantaneous IMEP method. It is thought that the teardown test still benefits from the highest popularity among OEMs, despite the fact that it is known to exclude the effect of the loading on the FMEP, and also the FMEP contribution coming from the interaction of components.

The method which captures all friction phenomena is the fired indicating method. This method entails an engine coupled to a dynamometer, and fired steady-state testing is done at certain speeds and loads. The IMEP is determined through the indicator diagram, whereas the BMEP is obtained in a conventional manner, usually using a load cell. Large uncertainty magnitudes in the FMEP are inevitable when using this method, especially with modern engines which have very high power densities and highly optimized mechanical friction. Mauke [3] explains how in modern engines, 1.1 % uncertainty in the measured IMEP can lead up to 33 % uncertainty in the FMEP determination. This can be understood through a simple uncertainty propagation analysis. Mauke [3] also explains how a 1.1 % uncertainty in the IMEP measurement is not unusual to encounter, and can be reached if just considering the thermal shock on the in-cylinder pressure sensor, and the uncertainty associated with the angular phasing of the in-cylinder pressure signal to TDC. Another limitation of the fired indicating method is that combustion induces variability on the testing, which consequently reduces the robustness of the FMEP determination.

A test which presents some of the answers to the discussed shortcomings is the conventional motored testing. This allows an FMEP measurement similar to the fired indicating IMEP method, but in the case of conventional motoring, the IMEP and BMEP are both small and comparable to the FMEP. This means that the FMEP can be determined with smaller deviations. Also the apparatus required to measure the BMEP can be downsized accordingly to measure over a smaller range, and hence have a greater resolution. This method also comes with the advantage of having very high repeatability due to the elimination of the variability of combustion. Unfortunately however, conventional motoring is usually criticized over the lack of load sensitivity on the FMEP, and also due to low in-cylinder temperature.

Due to the discussed shortcomings in both fired and conventional motored testing, a study was done at University of Malta on an experimental method known as 'Pressurized Motoring', or 'Motoring with External Charging'. This method consists of an engine driven with an electric motor, and also having its intake manifold pressurized, conventionally using air. Through the compression stroke, peak in-cylinder pressures synonymous to the firing operation can be obtained. This presents a setup which is able to impose the effect of speed and load on the FMEP, while still retains the advantage of a motored test, i.e. the repeatability, and small uncertainty propagation. This method was compared to the fired indicating method, the Morse test and Willan's line in [5] and showed that it presents a more advantageous trade-off between the conventional motoring FMEP testing and the fired indicating method. In [5], a shunt pipe was used between the intake and exhaust manifolds to recirculate the air, decreasing the power requirement of the pressurized air supply. It was also shown that with the use of this shunt pipe, the engine still retained thermal equilibrium throughout the testing session, i.e. no thermal runaway.

Allmaier [6] and MAHLE [7] highlight another advantage of the pressurized motored test which is that the in-cylinder temperature is independent of the load. This can be understood through a simple calculation using the equation of state, referenced to the intake valve closure. This means that it allows investigation of the FMEP at different speeds and loads, but at a relatively constant in-cylinder thermal condition.

In the conventional pressurized motoring using air, the in-cylinder temperatures are usually low, and similar to conventional motoring. This received criticisms [4] because low temperatures do not represent the FMEP contributions coming from thermal expansions and different oil film viscosities. To address this limitation, Argon was used in place of air as the working fluid, and in-cylinder temperatures synonymous to combustion were obtained [8].

Using Argon in place of air, also addressed another limitation of the pressurized motored testing - that of having large pumping losses, when compared to the equivalent fired condition [4]. This happens because in conventional pressurized motoring using air, the fired-like peak in-cylinder pressure is obtained by trapping more air in the cylinder on the intake stroke. This results in high pumping losses. When using Argon however, due to its high ratio of specific heats, the fired-like peak in-cylinder pressure can be obtained with smaller trapped mass. This showed that if Argon is used, pumping losses similar to that of an equivalent fired engine can be obtained.

Mixtures of gases between air and Argon were also synthesized and used as the working gas in the engine [9, 10] to investigate the relationship of FMEP with respect to gradually varying thermal conditions. The gas mixtures tested consisted of a range of ratio of specific heats varying between 1.4 (corresponding to air) and 1.67 (corresponding to pure Argon). It was found that in the pressurized motored engine, no measurable difference in FMEP was seen when the peak in-cylinder temperature was varied from 500 °C to 1200 °C, at two peak in-cylinder pressures being 84 bar and 103 bar, and a range of speeds varying from 1400 rpm to 3000 rpm. This result was somewhat troublesome to understand, however it is best understood if compared to results published by MAHLE [7] and Allmaier [6].

It was stated in [7, 6] that when comparing fired FMEP to pressurized motored FMEP using air, at similar speeds and peak in-cylinder pressures, the FMEP showed different trends, but comparable magnitudes. The authors attributed this difference to the thermal discrepancies arising from the two setups. From the data published in [9, 10] on the pressurized motored method, it was shown that a wide increase in in-cylinder temperature yielded no difference on the FMEP, which therefore means that temperature alone does not explain the difference between the fired FMEP and pressurized motored FMEP. It is thought that the different in-cylinder pressure curve shapes and the interaction of temperature, collectively, are responsible for the difference between the fired and pressurized motored FMEP.

It should be reminded that the pressurized motored method, both the conventional version using air, but also with the use of Argon, suffers from the limitation that the peak in-cylinder pressure is located in a relatively fixed position, at around 1 DegCA BTDC. On the other hand, for a fired engine, the location of peak pressure (LPP) is at around 10 DegCA ATDC for CI engines, and around 20 DegCA for SI engines. At these different locations of peak pressure, the piston velocities differ; where it is close to stationary for the pressurized motoring, and with an appreciably higher velocity for firing. This means that at the location of peak pressure, the motored engine might exhibit a higher tendency to boundary lubrication, whereas at the location of peak pressure for the fired engine, a more hydrodynamic lubrication might exist. This creates different dependencies of the FMEP on the lubrication viscosity, and consequently oil film temperature.

Another difference which arises at the two different locations of peak pressures is the connecting rod inclination. At the LPP corresponding to the pressurized motored case, the connecting rod is virtually vertical, which therefore limits the lateral thrust between the piston and cylinder wall. On the other hand for the fired case, the connecting rod inclination is appreciable, which therefore induces a higher lateral thrust between the piston and cylinder wall.

Based on the foregoing discussion, this study presents a one-dimensional simulation study which aims to assess the possibility, viability and extent of a modification to the conventional pressurized motored method (i.e. using air). This modification should allow a gradual variation of the location of peak in-cylinder pressure at fixed engine speeds and peak in-cylinder pressures. This method is aimed at bridging the pressurized motoring and pure firing, and hence dedicated at providing an FMEP measurement test with a large testing spectrum (i.e. several LPPs) at which FMEP can be obtained. Having a test which allows the experimental engine to be tested at a wide spectrum of conditions can provide benchmark results against which the widely known FMEP models can be tested and validated.

It is thought that having this method should retain the benefits of a pressurized motored engine, i.e. small uncertainty propagation, and good repeatability, but also provides an FMEP measurement which is closer to the FMEP of the fired engine by replicating the peak in-cylinder pressure magnitude, its location, as well as the in-cylinder temperature.

Engine Geometry and Proposed Setup Modifications

The idea proposed and simulated here includes very small quantities of fuel in the pressurized motored engine cylinders, whilst retaining the shunt pipe between the intake and exhaust manifolds, as well as motoring of the engine through the electric drive, where necessary. This consequently requires some bleed-off of exhaust from the system, as well as a make-up of fresh air to provide the necessary oxygen to sustain combustion and retain the desired peak in-cylinder pressure.

It should be reminded that, the location of peak in-cylinder pressure in a motored engine takes a position of 1 DegCA BTDC because of the heat and blow-by losses [11]. Therefore, theoretically, the addition of a small fuel quantity should make up for the losses of heat and blow-by from the cylinder, while the engine would still require motoring by the electric motor. This supposedly shifts the LPP further close to TDC. If the fuel quantity is increased further, the engine supposedly starts gradually supplying positive power and shifting the LPP to positive values. This new method being simulated shall be referred to 'fuelled pressurized motored' so as to make a clear distinction from conventional pressurized motoring, and also from a conventionally fired engine.

The simulation study aims to accept or reject the discussed hypothesis, and if proved possible, supply enough data which makes it possible for a researcher to replicate this study on an experimental setup. Hence, in developing this work, the difficulties that can be faced in experimental testing (possible O_2 deficiency, thermal runaway and control) were kept in sight in order to prevent suggesting any experimentally unpractical modifications.

To keep the experimental test as simple as possible, it was thought that minimal changes to the original pressurized motoring test setup would be ideal. As a result, the only three modifications which are being proposed are; a bleed valve at the exhaust side of the shunt pipe, the OEM common rail injection system (which for pressurized motoring might have been removed), and an engine control unit (ideally programmable, to allow flexible control of the fuel injection). It should be said that for the conventional pressurized motored setup, a bleed valve would already be present at the shunt pipe so that an accurate MAP can be imposed. Figure 1 shows the proposed setup for the fuelled pressurized motoring method.

Since the simulation study was done on a CI engine, diesel fuel was used in this study. This is believed to provide further simplifications if this proposed method had to be employed experimentally. This is due to the fact that CI combustion has

FIGURE 1 Schematic of the proposed modified pressurized motoring setup, still retaining the shunt pipe and electric drive, but having the OEM injectors, ECU and bleed valve.

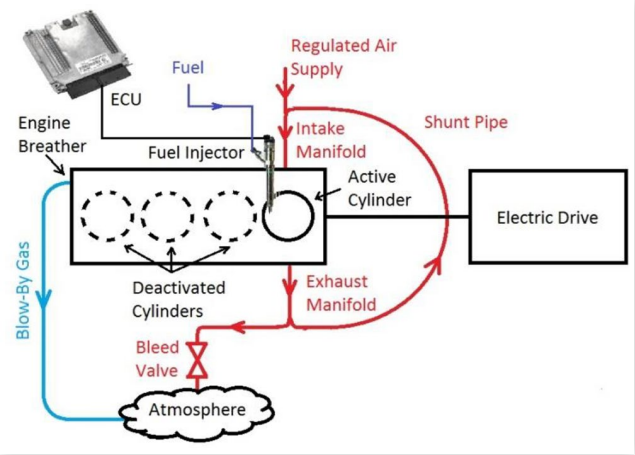

a coefficient of variation (COV) which is smaller than that for SI combustion. Other advantages include the high lambda tolerance and ability to withstand high peak in-cylinder pressures, which therefore allow for a wider testing spectrum.

Simulation Brief

In this work, a one-dimensional simulation study was favored for the exploration of this new method since it gives an indication of the likely gains to be made and avoids costly damage to the hardware. It allows flexibility of carrying out a multi degree of freedom study whilst giving relatively good basis for a qualitative deduction at a moderate computational time. In addition, it eliminates any variability which might hinder qualitative comparisons.

The simulation model was built in "GT-Suite" a commercial software used for 1D engine thermo-fluid analyses. The geometry of the engine considered in this simulation work was matched to that of the compression ignition engine used in [5, 8, 9, 10] in order to be able to make necessary comparisons with experimentally obtained data. To reflect the latest experimental setup at the time of writing, the engine was considered to be a single cylinder. The engine specifications are given in Table 1. While originally intended to have fixed burn profile, it became clear that the "feedback" aspects of the engine setup, such as variations in composition and thermodynamic state of the trapped gases in the cylinder setup, required a semi-predictive diesel combustion model available in the software package (DIPulse) to react accordingly. The combustion model required a look-up of injection profiles reflecting the solenoid common rail injection employed on the standard engine. Combustion/injection sub-models used had nominal coefficients representative of the CI engine on the test bed.

In developing the simulation model, the heat transfer was computed through the model presented by Woschni because it was considered the most suitable to deal with motored conditions since this was originally developed on both motored and fired engine cycles [12, 13].

To predict the likely BMEP, a mechanical friction model had to be chosen. The "Chen Flynn" model was selected for its piston speed and cylinder pressure sensitivity [14].

The setpoint parameters in this study were the engine speed and the magnitude of the peak in-cylinder pressure (PCP). A gradual variation of LPP was explored for each of the six tested setpoints shown in Table 2. The control variables to reach the aim of this test were four: the air supply pressure, the injected fuel quantity, the injection phasing, and the bleed valve restriction. To reduce the degrees of freedom, only one injection was used at a fixed rail pressure.

Prior to running a simulation matrix, manual variations of the presented four control variables were conducted to have a rough indication of the importance, sensitivity and magnitude of each variable. It transpired that the bleed valve restriction required having relatively small magnitudes in the range of 4 mm to 7 mm. It was also discovered that for a particular setpoint of engine speed and load, a variation of the bleed valve restriction was not really necessary; however a change was necessary between different setpoints. The constant bleed valve restriction for each setpoint considered was determined by observing the condition for the largest injection quantity and most advanced injection, since this condition showed the highest tendency for the engine to be starved of oxygen needed for combustion.

Having seen that the bleed valve restriction can be retained constant at a given setpoint of speed and PCP, the control variables were effectively decreased from four to three, i.e. injection quantity, injection phasing and air supply pressure. This made the simulation work simpler, and should also provide an easier control in the equivalent experimental tests.

The simulation campaign was made up of three sub sections:

- 2 speeds/3 PCPs at fixed bleed valve diameter, with a matrix of injected quantity and phasing (Table 2)
- A bleed diameter sweep for a fixed engine speed, PCP, Injected quantity and Injection phasing. This enabled the role of the bleed valve to be investigated.
- A comparison between pressurized motoring (air only), fuelled motoring and regular firing at a given speed, PCP and LPP. This drew a broader picture of the proposed method under study.

In the following section, the results obtained from the simulation matrices will be discussed.

TABLE 1 Engine specifications

Make and Model	Peugeot 306 2.0L HDi
Year of Manufacture	2000
Number of Strokes	4-stroke
Number of Cylinders	4, active 1
Valvetrain	8 Valve, OHC
Static Compression Ratio	18:1
Engine Displacement [cc]	1997
Bore [mm]	85
Stroke [mm]	88
Connecting Rod Length [mm]	145
Intake Valve Diameter [mm]	35.6
Exhaust Valve Diameter [mm]	33.8
Intake Valve Opens (1mm lift)	10 CAD ATDC intake
Intake Valve Closes (1mm lift)	20 CAD ABDC intake
Exhaust Valve Opens (1mm lift)	45 CAD BBDC expansion
Exhaust Valve Closes (1mm lift)	10 CAD BTDC exhaust

TABLE 2 Simulation points run with simulation matrices

Simulation Test Points		Peak In-Cylinder Pressures [Bar] 80	120	160
Engine Speed [RPM]	1400	✓	✓	✓
	3000	✓	✓	✓

Simulation Results - Part One: Injection Quantity and Injection Phasing at a Fixed Engine Speed and PCP

The data generated from the simulation matrices is relatively extensive, but following similar trends between different setpoints. The following discussion will be limited only to the setpoint of 3000 rpm; 80 bar, unless stated otherwise.

Magnitude and Location of Peak In-Cylinder Pressure

Figure 2 shows the graph of in-cylinder pressure against crank angle, with particular focus around the peak. It is noted that with different combinations of injection quantity and injection phasing, a positive shift of LPP up to around 9 DegCA was obtained. This shows that the initial hypothesis made in this work, i.e. that of shifting the LPP was shown to be possible through the proposed strategy of injecting small quantities of fuel. This is not to be confused with conventional firing operation, as will be made clearer in forthcoming figures.

At some conditions of injection quantity and injection phasing, a double peak pressure was observed, where the early peak belongs to the compression peak, and the late peak belongs to the combustion. The nomenclature used throughout this work is defined according to Figure 3. The foregoing observation of double-peak can be seen in Figure 4. This observation was also seen on the conventional-fired experimental HDi engine in [5], during an injection phasing sweep that was conducted on a water-brake dynamometer. It was observed experimentally that with a retarded start of injection (SOI), two peaks were visible (as in Figure 4), where in extreme cases, the combustion peak was lower than the compression peak. Advancing the SOI shifted the combustion peak closer to the compression peak, and also increased the magnitude of the combustion peak above that of the compression peak, such that the compression peak was no longer visible. Advancing the SOI extremely resulted in engine knock (or more broadly "very rapid combustion"). For reference purposes, throughout this publication, the curves with a single peak as shown in Figure 2 will be referred to as condition A. Condition B will refer to the case in which the compression peak and combustion peak are separate, and at the same magnitude. This condition is highlighted in Figure 4. Condition C will refer to the case where combustion peak is very late, and smaller in magnitude than the early compression peak. This condition is highlighted in Figure 4.

In this simulation work, the PID controller used to regulate the peak in-cylinder pressure was a simple one, which

FIGURE 2 The graph of peak in-cylinder pressure against crank angle showing the shift of LPP with different injection conditions.

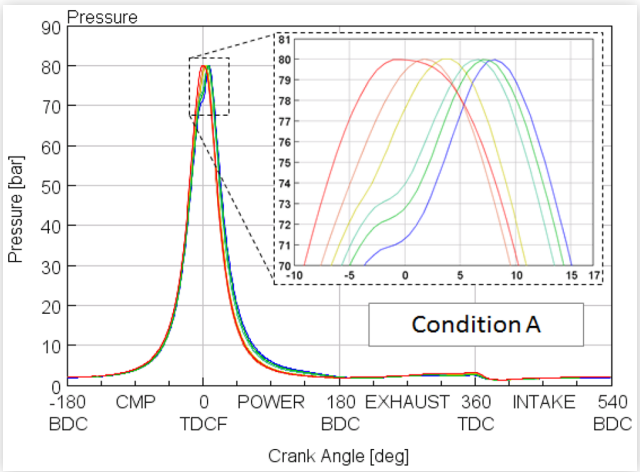

FIGURE 3 The nomenclature used throughout the paper to distinguish between the early compression peak and late combustion peak.

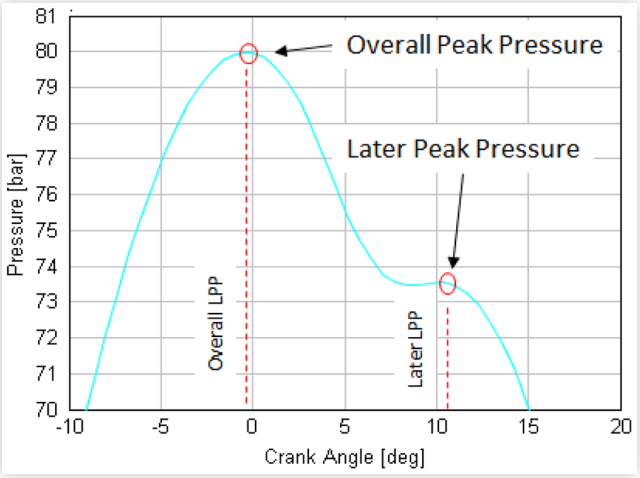

FIGURE 4 The graph of peak in-cylinder pressure against crank angle showing the conditions where the combustion peak is very late, and lower than the PCP setpoint.

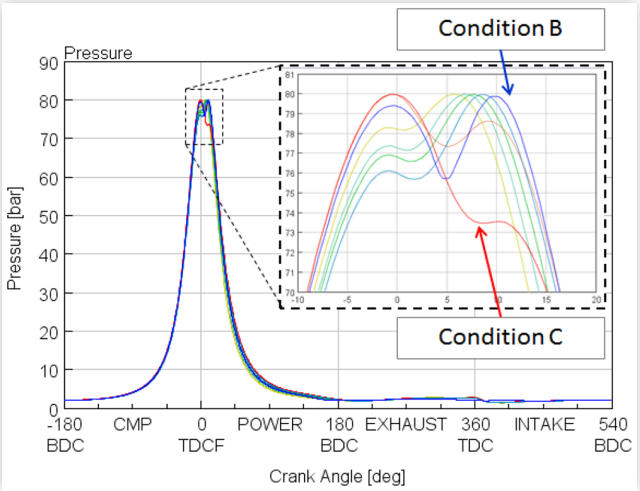

did not have the capability of distinguishing between the compression and combustion peaks. This means that in some of the curves shown in Figure 4 (condition C), the 80 bar compression peak was the one picked by the PID controller. Therefore these curves manifest an LPP at -1 DegCA, due to the compression rather than the other localized peak due to combustion. Even though this operating condition is not one which is very common in normal engine operation, it is thought that it still provides a useful asset to friction testing, as it gives a wider spectrum of loading characteristics. Furthermore, it should be appreciated that FMEP dependency on load is not explained solely by the peak in-cylinder pressure. The peak in-cylinder pressure is merely a convenient terminology which broadly describes mechanical loading, however the FMEP for the whole engine cycle is dependent on the pressure load-to-piston velocity phasing throughout the whole 720 DegCA cycle. This means that even if the fuelled pressurized motoring method is operated at 'condition C' with a peak pressure that is not exactly similar to that of the fired engine, it still gives a good resemblance of the fired-load throughout the expansion stroke.

Figure 5 shows a contour of the LPP obtained at the different combinations of injection quantity and injection phasing. It is noted how retarding the SOI and increasing the injected quantity yields in a gradually increasing positive shift in the LPP up to around 9 DegCA ATDC. Retarding the SOI further than -4 DegCA resulted in an abrupt decrease in the LPP shift, back to 1 DegCA BTDC. This result is due to the double peaking phenomena explained earlier, and termed 'condition C'.

To have a better understanding of the double peak observation, Figure 6 shows the location of the late peak. It can be noted that the LPP in Figure 6, for SOI more advanced than -4 DegCA are similar to those of Figure 5. This is due to the fact that for the cases in which a double peak was not shown, the overall peak is the same as the late peak, as in condition A. This is further explained by Figure 7 which shows the angular difference between the early compression peak and the late combustion peak.

This foregoing discussion can be further understood from Figure 8, which shows that for SOI more advanced than -4 DegCA, the late peak has a magnitude of 80 bar, which corresponds to the setpoint pressure. On the other hand, for SOIs which were retarded more than -4 DegCA, the late peak magnitude was lower than 80 bar. This is due to the fact that for these conditions, the 80 bar was reached by the early compression peak, and not by the late combustion peak, as in condition C.

It is noted that multiple in-cylinder pressure maxima can/do appear and it is purely for consistency with literature that we are using the metric 'LPP'. Other metrics maybe an "effective angle, the pressure center, integrated over the crank angles might be more appropriate"

FIGURE 5 The contour showing the overall LPP.

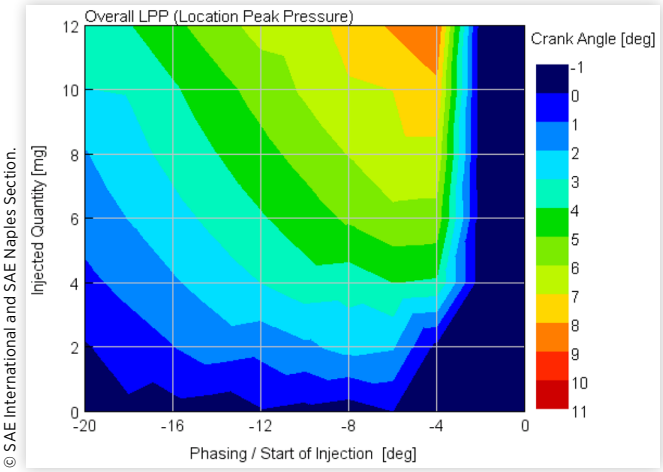

FIGURE 6 The contour showing the LPP for the late peak.

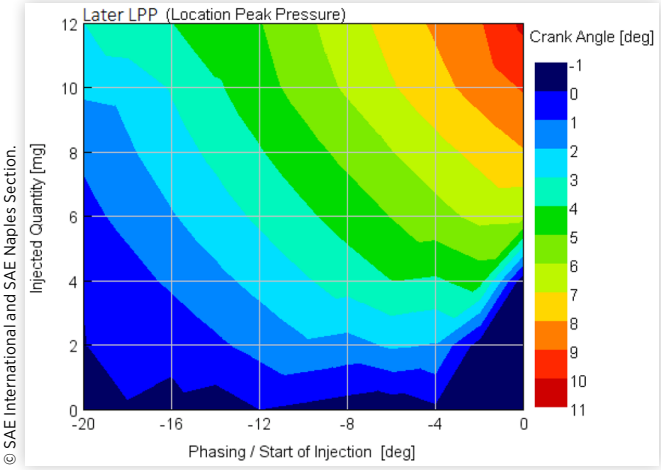

FIGURE 7 The contour showing the angular difference between the early and late peak in-cylinder pressures.

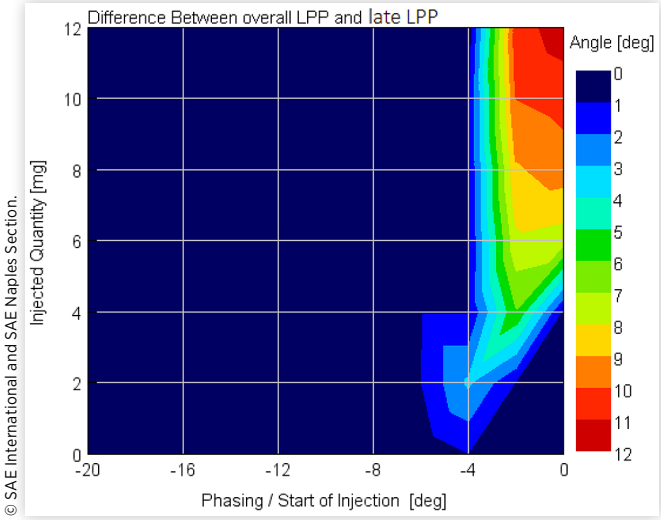

Intake Manifold Pressure, Air Supply, and Volumetric Efficiency

With the proposed method of fuelled pressurized motoring, since small quantities of fuel are introduced in the cylinder, some consumption of the pressurized fresh air occurs. In this

FIGURE 8 The contour showing the magnitude of the late peak in-cylinder pressure.

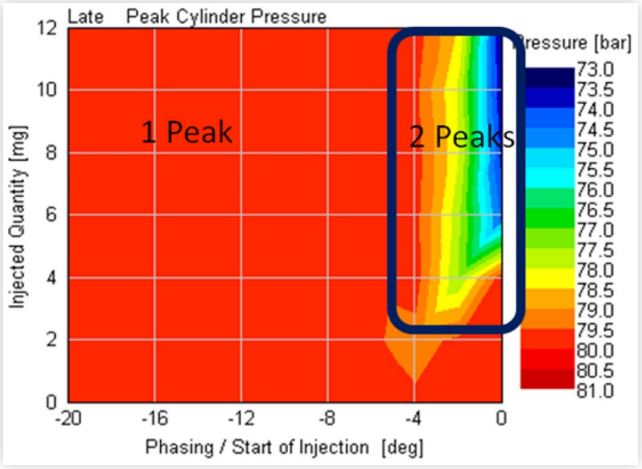

simulation study, the exhaust gases were partially bled off from a small diameter bleed valve connected to the exhaust manifold. As a consequence, fresh air had to be replenished through a regulated air supply. The air supply is required to have pressures above atmospheric conditions, similar to that in a conventional pressurized motored engine, in order to be able to reach the desired peak in-cylinder pressure. Figure 9 shows the intake manifold pressure required to obtain the discussed setpoint of 80 bar, at 3000 rpm. When observing this figure, it should be kept in mind that the gas present in the intake manifold is a mixture of fresh air and recirculated gas, which is also a mixture of unburnt air and exhaust. Figure 9 shows that increasing the fuel injection quantity and advancing the SOI required a smaller manifold pressure. It can be noted how the conventional pressurized motored situation (i.e. at 0 mg of fuel) requires a much higher manifold pressure. This observation is consistent with theory, in the sense that, with conventional pressurized motoring, the peak in-cylinder pressure is a result of a higher trapped mass, whereas in this communicated method, the compression peak pressure is amplified with the energy released by the minor combustion. Generally speaking, a higher fuel quantity requires a lower compression pressure, and therefore lower manifold pressure.

Even though not presented here, it was observed that increasing the fuel quantity and retarding the combustion increases exhaust manifold temperature, which by recirculation through the shunt pipe, increases the intake manifold temperature, and therefore lower gas density. This would in turn require a compensating higher intake manifold pressure.

The intake manifold oxygen concentration was also studied, but not shown in this publication. The lowest oxygen concentration occurred at the highest injection quantity and earliest injection phasing, and found to be 15% by mass. On the other hand, the highest oxygen content was under motoring condition, where a 23% mass concentration was noted, i.e. corresponding to atmospheric air. It is highlighted that the values of oxygen content being communicated are only indicative. This is due to the fact that they are largely dependent on the bleed valve restriction that was set before running the simulation matrix.

In a previous publication by the same authors [5], the air supply pressure and flow rate required for a conventional pressurized motored engine (using air) was found to be minimal. This was highlighted as being one of the advantages of using the pressurized motoring since a normal shop floor compressor can be used. The supply flow rate requirement was reduced even further during Argon and mixtures studies, when the blow-by from the engine was re-routed back to the shunt pipe via a small refrigeration compressor to retain a closed system. As a result, the supply mass flow could be sustained throughout the test matrix from a 10 Nm^3, 200 bar cylinder. [8]

In this work, since fuel is added to the system, and exhaust is bled off, a study of the consumption of pressurized air was fitting to assess the compressor size required to run the engine with the proposed strategy. Figure 10 shows the air supply flow rate at the respective manifold pressures, shown previously in Figure 9. The data from both these figures show that despite the exhaust bleed off, a considerably small compressor should keep up with the air supply required. Figure 11 shows the fluid delivery power at the discussed condition of 3000 rpm and 80 bar. The fluid power requirement increases with a

FIGURE 9 The contour of intake manifold absolute pressure.

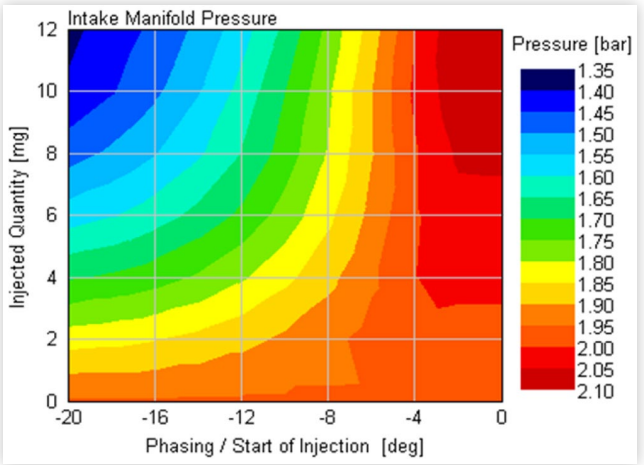

FIGURE 10 The contour of the air supply mass flow rate.

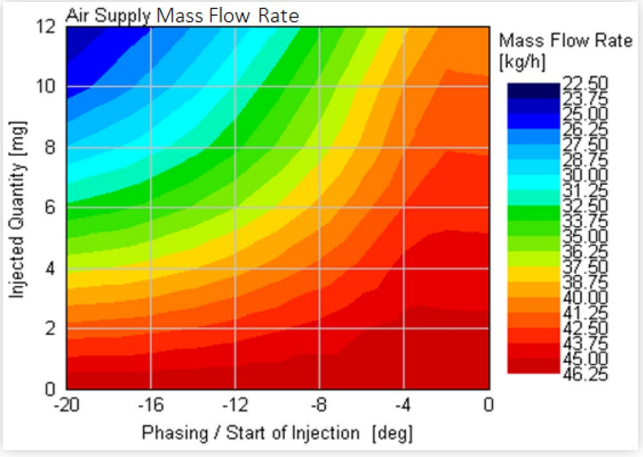

FIGURE 11 The contour of fluid power.

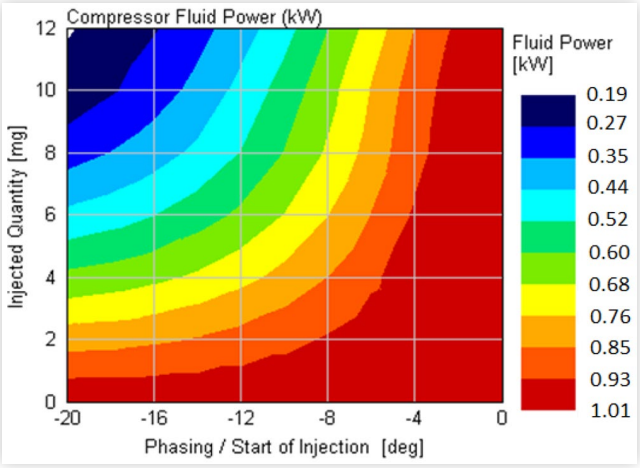

decrease in the fuel quantity, up to a maximum of 1.01 kW. While initially counter-intuitive, this trend is one which can be relatively easily understood. It results because a decrease in the fuel quantity requires a higher compression pressure, and hence a higher delivery flow-rate at a higher manifold pressure to obtain the setpoint peak in-cylinder pressure. It should also be mentioned that due to the bleed valve restriction being a fixed value, higher manifold pressures meant a higher bleeding flow rate, which consequently had to be replenished from the fresh air supply system.

The volumetric efficiency is defined by Livengood [15] as the ratio of the volume of total dry gas taken in by one cylinder on one suction stroke (at inlet density) to the piston displacement of the cylinder. It was found that the volumetric efficiency of the engine increases with injected quantity from 90 % to 93 %. This slight change in the volumetric efficiency can be attributed to at least two factors.

The first cause might be that increasing the fuel quantity, and hence the heat release, results in a consequent increase in the exhaust blow down (hence better exhaust scavenging, and consequently better volumetric efficiency). This exhaust blow down effect decreases with a decrease in the fuel injected quantity, and is totally missing for the conventional pressurized motored case (i.e. no injected fuel condition). Actually, in conventional pressurized motoring, the opposite of blow down occurs; as soon as the exhaust valve opens, gas from the shunt pipe enters the cylinder due to the fact that heat and blow-by losses throughout the closed part of the cycle would have decreased the in-cylinder pressure at EVO, when compared to the in-cylinder pressure at IVC (or shunt pipe pressure).

The second observation which explains the variation of volumetric efficiency is the relationship with the intake manifold temperature. It was seen (but not presented here) that the intake manifold temperature increased from around 52 °C to around 85 °C, with an increase in injection quantity from 0 mg to the maximum of 12 mg. The intake manifold temperature showed minimal decrease with a retardation of the injection. The volumetric efficiency is therefore perfectly coherent with the variation of the intake manifold temperature, according to the well-known square root law [16, 15].

Mean Effective Pressures

This section deals with the presentation of the simulation results for the indicated, pumping, brake and friction mean effective pressures. Figure 12 shows the IMEPnet for the discussed setpoint of 3000 rpm and 80 bar. It should be reminded that for a motored engine, the IMEP net is a measure of the heat losses, blow-by losses, and pumping losses. For a fired engine, on the other hand, it represents both the work done by the combustion gases, and the losses from the cylinder. At the point corresponding to 4 mg of fuel, the heat, blow-by and pumping losses are being supplied through the energy released from the combustion. Increasing further the injected quantity results in a positive IMEPnet which indicates excess heat release that is able to do work against the piston. It should be noted that comparing the IMEPnet at the 0 mg condition from Figure 12 to that obtained at the same condition of PCP and engine speed, with air in [9], for the same engine but of the four cylinder version, shows a very good correlation.

For a good appreciation of the previous observation on the IMEPnet, Figure 12 should be seen in conjunction with Figure 13 for the BMEP. The BMEP for a pressurized motored engine (0 mg of fuel injection) represents the work done by the driver (usually an electric motor) to motor the engine, or in other words make up for the engine losses i.e. heat and blow-by losses, pumping losses, friction losses, and any accessory losses if present. In this case, no accessory losses were assigned. Therefore the only difference between Figure 12 and Figure 13 is the FMEP, as computed from the Chen and Flynn model, available in the simulation software. It can be seen from Figure 13 that the BMEP shows minimum net mechanical work for the case of 0 mg of fuel, and the net work done increases with an increase in injection quantity. At around 7 mg of fuel injection (denoted by the dashed line in the figure), the BMEP is zero and increases to positive values at injection quantities higher than 7 mg.

The transition from negative to positive values of BMEP shows that the combustion happening in the engine first makes up for the losses of the engine, and then starts supplying

FIGURE 12 The contour of the IMEPnet. Dashed line shows zero IMEP.

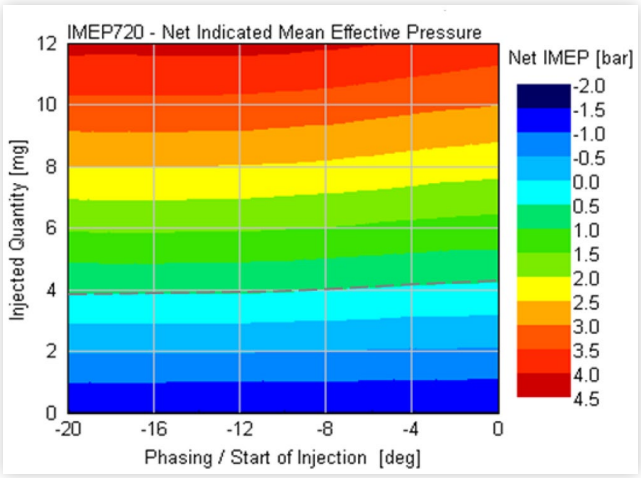

FIGURE 13 The contour of the BMEP. Dashed line shows zero BMEP.

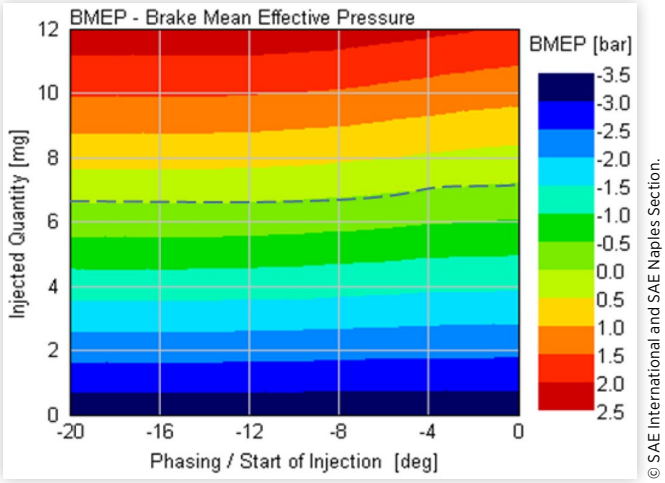

FIGURE 14 The contour of the PMEP

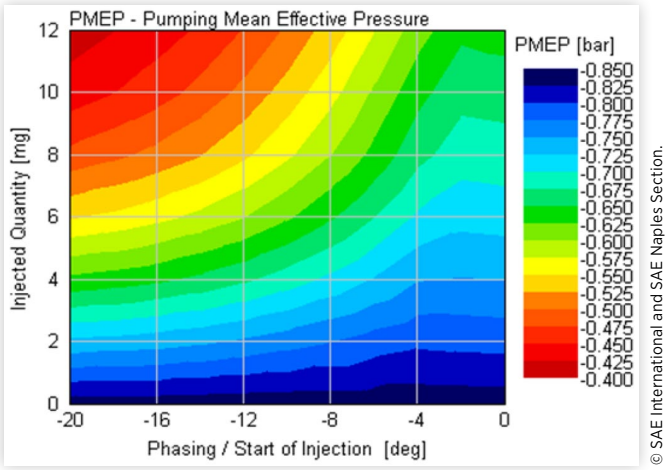

some net positive work, if the fuel quantity increases. This observation shows that the electric motor driving the engine at negative BMEP values must be capable of absorbing power at positive BMEP values. When comparing Figure 13 to Figure 12 it can be seen that the zero IMEPnet occurs at a different injection quantity than for the zero BMEP condition. The zero BMEP requires an additional 3 mg to 4 mg of fuel injection, when compared to that required at the zero IMEP. This difference in the two graphs is due to the additional energy required to overcome the FMEP.

The zero BMEP observed at 7 mg of fuel hints that at this single condition, the engine is not providing useful work, but neither requiring an external driver. In other words, this is a condition in which the energy released by combustion is just enough to supply all the losses of the engine, such that the engine is self-sustaining. This is synonymous to the condition of 'idling', however with this method this condition can occur at all engine speeds and all peak in-cylinder pressures. This observation is one of interest for engine testing, and will be discussed in greater detail in the forthcoming discussion section.

The pumping mean effective pressure is given in Figure 14. It is shown that the PMEP is a negative value throughout, meaning that it is always a loss of energy. The pumping loss increases when going from the maximum injection quantity to the conventional pressurised motored case at 0 mg. This observation is well understood and attributed to the fact that going towards the pressurized motored case requires a higher trapped mass to obtain the same peak in-cylinder pressure magnitude. A higher trapped mass requires more pumping effort, and hence a higher pumping loss. An increase in pumping losses is also seen when retarding the fuel injection. Comparing the value of the PMEP obtained in this work for the pressurized motored case, to that recorded experimentally at the same engine speed and PCP, with air in [9] shows a very good correlation. The experimental value recorded at 3000 rpm and 84 bar peak in-cylinder pressure was -0.72 bar.

The FMEP as computed through the Chen-Flynn sub-model was found to be constant with engine speed, and equal to 1.80 bar throughout the variation of injection quantity and injection phasing. This is something which is expected since the piston speed and the peak pressure are maintained constant throughout the simulation test matrix. The corresponding experimental testing to this simulation campaign will shed light on what the actual contour of the FMEP should look like. The Chen-Flynn friction sub-model can only give a constant approximate value since it is not able to detect thermal conditions and the location of peak in-cylinder pressure. As a result, the only useful information that can be obtained in this case from the result of the Chen-Flynn model is to roughly estimate the BMEP from the IMEP, and roughly obtain the condition at which point the engine shifts from requiring motoring into power absorbing. It should be noted that the FMEP obtained through the Chen and Flynn (1.80 bar) is still of the same order of magnitude as IMEPnet and BMEP, which means that the uncertainty propagation which results from the measurement uncertainty, is still relatively small.

FMEP Robustness Factor

Apart from obtaining firing-representative in-cylinder pressure and temperature, this work was also focused on improving the reliability and robustness of the FMEP measurement. A metric needs to be introduced which gives an idea of the uncertainty propagation magnitudes expected from the equivalent experimental FMEP data; the larger the ratio, the lesser the uncertainty propagation. The proposed metric which will be referred to in this paper is the 'FMEP robustness factor', and computed through equation (1).

$$FMEP\ Robustness\ Factor = \frac{FMEP}{max\left(abs\left(IMEPnet\right), abs\left(BMEP\right)\right)} \quad (1)$$

When computed, the factor essentially compares the magnitude of FMEP to the dominant magnitude of either IMEP or BMEP, whether positive or negative. This metric avoids the ∞ values at zero IMEP and BMEP, and varies

FIGURE 15 The contour of the FMEP robustness factor.

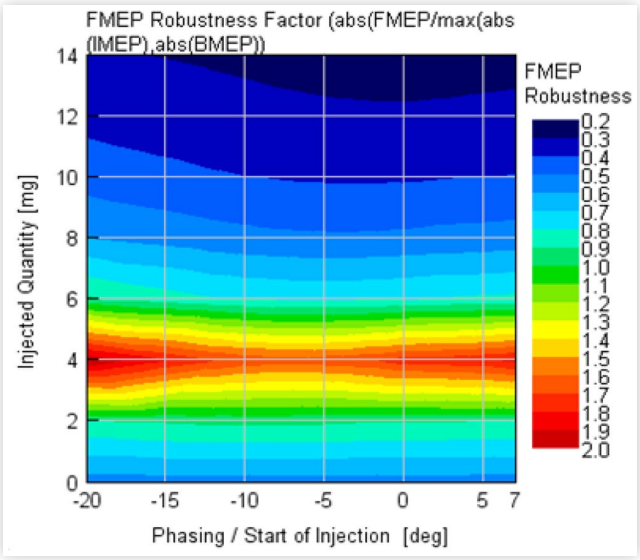

between zero and 2.0 (corresponding to the case when the magnitudes of IMEP and BMEP are equal and half that of FMEP). Figure 15 shows the FMEP robustness factor contour for the discussed simulation setpoint.

For the discussed condition of 3000 rpm and 80 bar, the FMEP robustness factor at the case of conventional pressurized motoring (0 mg) is equal to 0.5. Introducing fuel however resulted in FMEP robustness factor as high as 2. This means that introducing a small combustion, apart from making the FMEP measurement more realistic, and closer to the actual fired condition, it also enhanced the already mentioned and discussed advantage of the conventional pressurized motoring, i.e. that of having a small uncertainty propagation.

Bulk In-Cylinder Temperature

Figure 16 shows the in-cylinder peak bulk gas temperature predicted by the simulation. The method brought forward in this work addressed more than one limitation of the pressurized motored method. Through the minimal quantity of fuel being added to the cylinder, apart from shifting the LPP to positive crank angles similar to actual fired conditions, peak in-cylinder temperatures synonymous to fired conditions were also obtained. It can be seen in Figure 16 that the bulk gas peak in-cylinder temperature varied from 650°C from conventional pressurized motored (i.e. using air with no fuel), to 1300°C at maximum injected quantity and most advanced injection. This variation trend is also synonymous to fully fired engines.

Previous publications by the same authors utilized a separate method to increase the in-cylinder temperature to fired-like magnitudes. This involved the use of Argon, and its mixtures with air as the working fluid, instead of pure air [8, 9, 10]. It was observed experimentally that using Argon successfully resulted in obtaining fired like in-cylinder temperatures, high heat transfer rates, fired-like pumping losses, but constant mechanical friction losses. Using Argon, and its mixtures presents the advantage that apart from increasing the in-cylinder temperatures to fired-like values, it allows a relatively constant in-cylinder temperature trace with different engine speeds and loads. Due to this, it is appreciated that the method presented in [8, 9, 10] is not really a competitor to the method investigated by this simulation, but rather presents an alternative method with a different scope.

Heat Transfer

The sub-model employed for the heat transfer rate estimation in this simulation campaign was based on the Woschni correlation. This sub-model was chosen amongst others available since it was developed from both motored and fired engine data [13], and hence deemed the most appropriate. Figure 17 shows the average heat transfer rate predicted by the sub-model, which indicates that increasing the injection quantity resulted in an overall increase in the heat lost from the cylinder. A lesser dependency on the injection phasing is evident, which generally shows that advancing the injection results in a higher heat loss.

FIGURE 16 The contour of the in-cylinder peak bulk gas temperature.

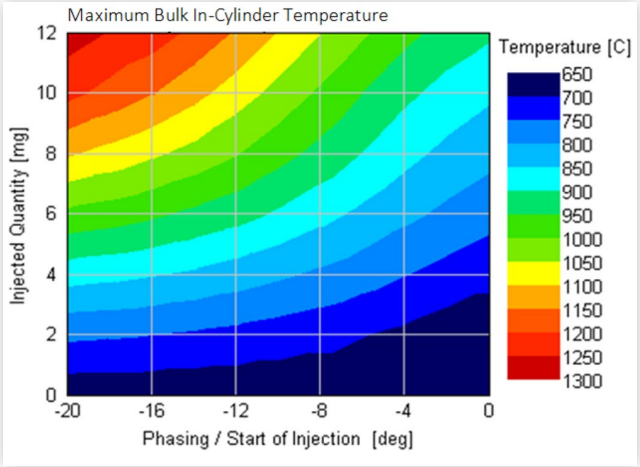

FIGURE 17 The contour of the in-cylinder heat transfer rate.

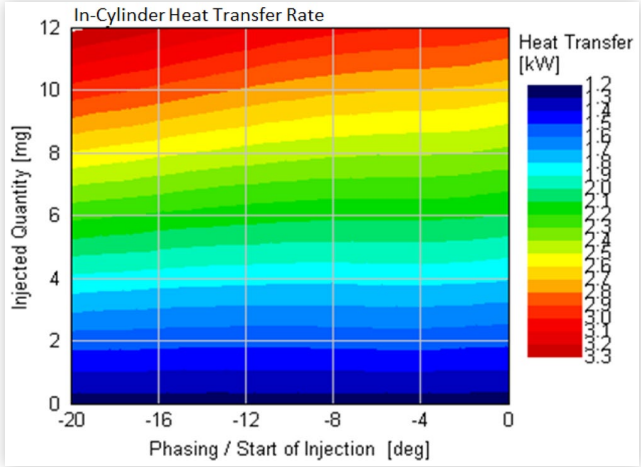

Other Simulated Setpoints

As discussed in an earlier section, a total of six setpoints were run with a simulation matrix. This means that the data presented for the case of the 3000 rpm, 80 bar was also analysed for five other setpoints. In general the same trends were shown for all setpoints. In order to reduce the amount of data presented here, the maximum and minimum values of the contours generated for all the six setpoints are presented in Table 3. Overall maximum and minimum values throughout all the setpoints of speeds and peak in-cylinder pressure are selected and given in the rightmost two columns. This is done to give the reader a sense of the range of variation that is to be expected. It is important to note that the maximum or minimum values of a parameter do not correspond to the maximum/minimum of another parameter. The intention is to only show the likely ranges expected from the experimental engine.

Throughout the setpoints simulated, the bleed valve restriction was set to values between 2.6 mm and 8.0 mm (as shown in line 3 of Table 3). As explained earlier, for every setpoint, the bleed valve was kept constant. It was noted that

TABLE 3 The maximum and minimum values for the six simulated test conditions. The max or min of a parameter does not correspond to the max /min of another parameter. The intention is to only show the likely ranges expected from the experimental engine.

			1400 80 Min	1400 80 Max	1400 120 Min	1400 120 Max	1400 160 Min	1400 160 Max	3000 80 Min	3000 80 Max	3000 120 Min	3000 120 Max	3000 160 Min	3000 160 Max	Min	Max
	Engine Speed	**rpm**	**1400**		**1400**		**1400**		**3000**		**3000**		**3000**		**1400**	**3000**
	Overall Peak Cylinder Pressure	**bar**	**80**		**120**		**160**		**80**		**120**		**160**		**80**	**150**
1	Injected Phasing	deg aTDC	-20	7	-20	0	-20	0	-20	0	-20	0	-20	0	**-20**	**7**
2	Injected quantity	mg	0	14	0	14	0	14	0	12	0	14	0	14	**0**	**14**
3	Bleed Valve Diameter	mm	7.0	7.0	3.8	3.8	2.6	2.6	8.0	8.0	6.0	6.0	5.0	5.0	**2.6**	**8.0**
4	Overall LPP	deg aTDC	-0.9	12.8	-0.7	6.7	-0.7	4.5	-0.7	8.9	-0.8	6.0	-0.7	4.1	**-0.9**	**12.8**
5	Later LPP	deg aTDC	-0.9	15.1	-0.7	7.1	-0.7	5.5	-0.7	10.2	-0.8	5.8			**-0.9**	**15.1**
6	Later PCP (Second Peak if applicable)	bar	65		118		154		73		118				**65**	**154**
7	Difference LPP	degCA	0.0	16.6	0.0	7.7	0.0	6.3	0.0	12.0	0.0	6.5			**0.0**	**16.6**
8	Max Cylinder Temperature	C	618	1440	636	1022	648	878	664	1273	690	1049	711	956	**618**	**1440**
9	50% Mass Burn Fraction	degCA	-11.0	15.1	-12.5	10.8	-12.7	13.0	-6.1	13.9	-8.9	17.5	-9.8	19.2	**-12.7**	**19.2**
10	10-90 Burn Fraction	degCA	5.5	14.4	11.3	30.7	12.7	40.9	7.7	23.6	13.1	41.4	15.1	47.9	**5.5**	**47.9**
11	Intake Manifold Pressure	bar abs	1.12	2.05	2.31	3.18	3.53	4.32	1.39	2.09	2.55	3.24	3.72	4.37	**1.12**	**4.37**
12	Intake Manifold Temperature	C	46	53	54	79	58	95	54	84	68	129	79	147	**46**	**147**
13	Intake Manifold O2 Mass concentration		0.16	0.23	0.14	0.23	0.12	0.23	0.15	0.23	0.13	0.23	0.12	0.23	**0.12**	**0.23**
14	Lambda		1.3	100	1.5	100	1.5	100	1.5	100	1.5	100	1.6	100	**1.3**	**100**
15	Air Supply Mass Flow Rate	kg/hr	10	37	10	16	7	10	24	46	27	39	28	35	**7**	**46**
16	Compressor Fluid Power	kW	0.03	0.82	0.25	0.60	0.28	0.45	0.19	1.01	0.76	1.32	1.13	1.61	**0.03**	**1.61**
17	Fresh Air to Total gas ratio		0.43	0.86	0.22	0.26	0.11	0.12	0.42	0.54	0.28	0.31	0.20	0.22	**0.11**	**0.86**
18	Volumetric Efficiency (manifold)		0.92	0.94	0.93	0.95	0.94	0.96	0.91	0.93	0.91	0.96	0.91	0.96	**0.91**	**0.96**
19	BMEP	bar	-2.42	3.75	-3.00	3.14	-3.58	2.53	-3.39	2.31	-4.25	2.23	-5.08,	1.45	**-5.08**	**3.75**
20	IMEP720	bar	-1.08	5.09	-1.50	4.64	-1.91	4.20	-1.55	4.15	-2.24	4.23	-2.90	3.63	**-2.90**	**5.09**
21	FMEP	bar	-1.34	-1.34	-1.50	-1.51	-1.67	-1.67	-1.84	-1.84	-2.01	-2.01	-2.17	-2.17	**-2.17**	**-1.34**
22	PMEP	bar	-0.28	-0.15	-0.38	-0.28	-0.50	-0.41	-0.84	-0.41	-1.24	-0.76	-1.63	-1.11	**-1.63**	**-0.15**
24	FMEP Robustness Factor		0.26	1.98	0.32	1.40	0.40	1.98	0.44	1.43	0.47	1.72	0.43	1.97	**0.26**	**1.98**
25	Brake Power	kW	-1.4	2.2	-1.7	1.8	-2.1	1.5	-4.2	2.9	-5.3	2.8	-6.3	1.8	**-6.3**	**2.9**
26	In Cylinder Heat Transfer Rate	kW	0.6	2.7	0.8	2.4	1.0	2.4	1.2	3.3	1.8	4.1	2.3	4.5	**0.6**	**4.5**
27	Exhaust Manifold Temperature	C	65	252	68	196	71	177	87	278	97	263	104	251	**65**	**278**

the bleed valve has a dominant role when some parameters do not go monotonic with speed and/or PCP. To investigate this further, another simulation was run, where the injection quantity and injection phasing were retained constant, and the bleed valve diameter was varied. The results from this simulation are discussed in the next section.

Table 3 shows the range for the LPP obtained for each setpoint (line 4 & 5). It can be seen that, overall, the maximum LPP obtained with this method was 12.8 DegCA ATDC. This occurred at the smallest condition of speed and PCP, i.e. 1400 rpm, 80 bar. It is noted that the achievable LPP range decreases with an increase in the peak in-cylinder pressure. It is thought that at higher pressures, the influence of the fuel (0-14 mg) diminishes and therefore the flexibility of the method is not equal under all setpoint conditions. The range of shifting in LPP can be seen in Figure 18. Fortunately the method is more flexible at lower peak in-cylinder pressures, where lower engine loads occur and the role of friction is more dominant in the energy balance of the engine.

Another interesting observation made from Table 3 is the peak in-cylinder temperature (line 8). The minimum values for this parameter correspond to the case of the 0 mg of fuel, i.e. the conventional pressurised motored case. The maxima vary between 878 °C and 1440 °C. This shows that relatively high temperatures, and in some cases synonymous to firing can also be obtained. Similar to this, it should be noted that both the intake and exhaust manifold temperatures also reached maxima as high as 147 °C for the intake side, and up to 278 °C for the exhaust side. Apart from its importance from a data analysis point of view, the manifold temperatures are also essential for the shunt pipe construction. In [5], the shunt pipe was constructed with a 270° bend from a 2 mm thick stainless steel tube. The 270° bend was split in two and connected through a rubber junction to avoid internal stress induced by differences in thermal expansions of the intake and exhaust manifolds. Due to the high temperatures expected with the fuelled pressurized motoring, the shunt pipe should be made up of materials which can withstand typical fired engine temperatures.

An interesting observation which was made in this simulation study is that for the pressurized motoring cases (no fuel), the exhaust manifold ended up being hotter than the intake manifold. This observation was also done in [5, 8, 9, 10] from

FIGURE 18 The graph of the range of LPPs at different peak in-cylinder pressure.

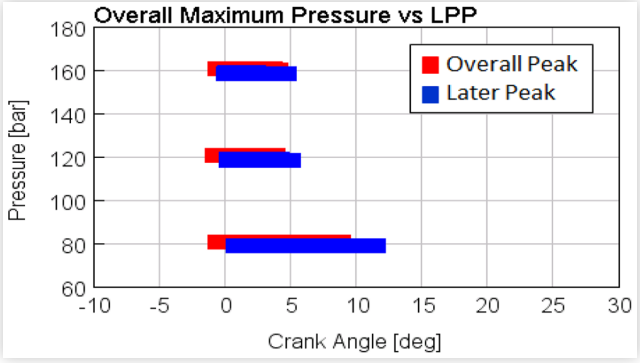

FIGURE 19 An indication of the FMEP robustness factor at 1 bar FMEP, for conventional pressurized motoring, fuelled pressurized motoring and fully fired.

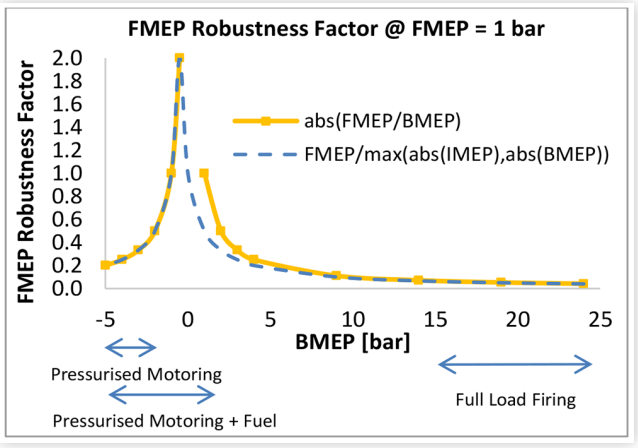

experimental results, which was initially troublesome to understand, due to the fact that the gas at EVO is theoretically colder than the gas at IVC, due to the heat losses during the closed part of the cycle. Another observation showed that during the exhaust stroke, for the conventional pressurized motored engine, a recompression of the exhaust gases occur. This was seen both experimentally and also through this simulation. It transpired that the two observations are related, which means that the recompression occurring due to a restrictive exhaust valve curtain area (and backflow at EVO from shunt pipe to cylinder), increased the temperature of the bulk in-cylinder gas on exhaust to values higher than the intake temperature. This explanation was obtained through this simulation, by assigning a multiplier for the exhaust valve area ranging from values of 1.0 to 1.4. It showed that at higher area multipliers, the exhaust temperature decreased by around 10 °C, hence proving that the previously troublesome measurement of high exhaust side temperature in the motoring condition is due to the restrictive exhaust valve.

Table 3 also shows the maximum value of fluid power requirement (line 16). This occurs at the condition of 3000 rpm, 160 bar at the condition of 0 mg of fuel. At this condition, the intake manifold pressure is 4 bar absolute. The corresponding fresh air mass flow rate is 35 kg/hr. These yield a maximum fluid power of 1.6 kW, which is thought to be a very reasonable value for an experimental setup (500cc engine cylinder).

The earlier introduced metric of FMEP robustness factor is also presented in Table 3 (line 24). In addition, to have a visual understanding of the FMEP robustness factor, Figure 19 is plotted which compares the cases of conventional pressurized motoring, fuelled pressurized motoring and fully firing. It can be seen how the FMEP robustness factor of the conventional pressurized motored method is already much better than that of the fully fired engine (fired indicating method). The fuelled pressurized motoring presents even better FMEP robustness factor.

Another observation made from Table 3 is that the 10% to 90% burn duration (line 10) is relatively short for some setpoints, such as the 1400 rpm, 80 bar. This indicates a very

fast burn which experimentally should yield a low coefficient of variation. It is also noted that the 50 % burn (line 9) has a wide range and is well within firing operation.

The maxima for the average heat transfer rate out of the cylinder ranged between 2.4 kW to 4.5 kW (line 26). This range of values is significantly higher than that for conventional pressurised motoring (using air only), which ranged between 0.6 kW and 2.3 kW. The versatility of this method on heat transfer measurements is yet to be explored, however in this table, the magnitude for heat transfer rate was included mainly to show that the fuelled pressurized motoring method can impose high heat transfer rates, which therefore moves away from the cold testing synonymous with conventional motoring.

According to the brake power values (line 25) given in Table 3, the electric motor coupled to the single cylinder engine, with a displacement of around 500 cc, had to generate a maximum of 6.3 kW and absorb a maximum of 2.9 kW. For an equivalent four cylinder engine, the power ratings are still small and manageable with a reasonably inexpensive motor.

Simulation Results - Part Two: Effect of Bleed Valve Restriction

As communicated in earlier sections, the results of the simulation matrices presented and discussed were run with a constant bleed valve restriction, but specific for each setpoint, as shown in earlier Table 3. This implies that to a certain extent, the data presented so far is only indicative, since it is dependent on the bleed valve restriction set for the particular test condition. One parameter which might have been affected by this is the flow rate of supply fresh air. To assess the extent to which the bleed valve restriction affects quantities discussed earlier, a separate simulation was run for the test condition of 1400 rpm, 80 bar, with a constant injection quantity of 14 mg and injection phasing of -4 DegCA BTDC. This particular test condition was chosen amongst others since it was observed that it is the one in which the method is more responsive to variations in control parameters. At this condition, the bleed valve restriction was varied from 2.5 mm to 5.5 mm.

As an initial indicator, Figure 20 shows the graph of in-cylinder pressure against crank angle. It is shown that increasing the valve diameter (i.e. decreasing the restriction) showed a positive shift of around 10 DegCA in the overall LPP. This can be better identified from Figure 21. An increase in the bleed valve diameter also resulted in an overall higher contribution from combustion to reach the required 80 bar of peak in-cylinder pressure. As a consequence, the compression pressure peak could be decreased. This observation is tied to the concentration of oxygen supplied to the cylinder, which shall be explained in the subsequent text. Note that in Figure 20, the left most curve has two peak in close succession, targeted to not exceed 80 bar pressure.

Increasing the bleed valve diameter resulted in higher oxygen content in the intake manifold and hence also in the cylinder, as shown in Figure 22. This means that a higher fresh

FIGURE 20 The in-cylinder pressure curve variation for a change in bleed valve restriction.

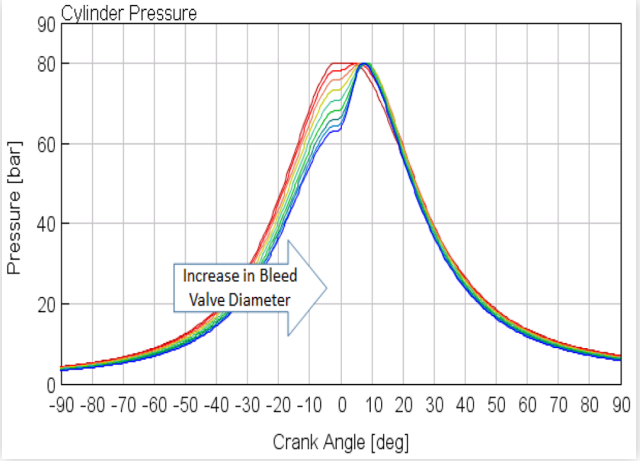

air mass flow had to be delivered by the air supply, but at a lower intake pressure, as given in Figure 23 and Figure 24. From these two quantities, the fluid power required for the different bleed valve diameters was found and presented in Figure 23. It can be seen that due to the higher mass flow rate of bleeding, an increase in the fluid power is required, with an increase in the bleed valve diameter. It should be said that even though a 40 % increase in the fluid power is required, the value of the fluid power is still small and equal to 0.2 kW.

Figure 25 shows that a larger bleed valve diameter resulted in a decrease in the combustion duration. This is attributed mainly to the relationship previously explained between oxygen content in the intake manifold and bleed valve diameter. Due to the rapid burn, a better coefficient of variation is achievable, compared to smaller bleed valve diameter, if the test is conducted on the experimental engine. The shorter combustion induced by the higher oxygen concentrations at larger bleed valve diameters, resulted in a higher contribution in the generation of the peak in-cylinder pressure, as explained earlier in Figure 20. Emphasis is made here on the usefulness of the injection /combustion sub-model to capture these oxygen concentration effects.

FIGURE 21 The overall LPP and IMEPnet at different bleed valve restrictions.

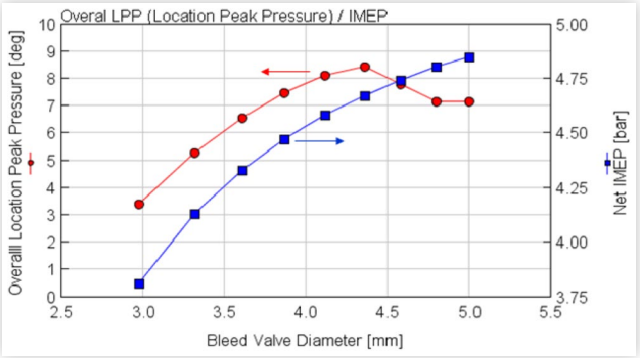

FIGURE 22 The oxygen concentration and peak bulk gas in-cylinder temperature variation with a change in bleed valve restriction.

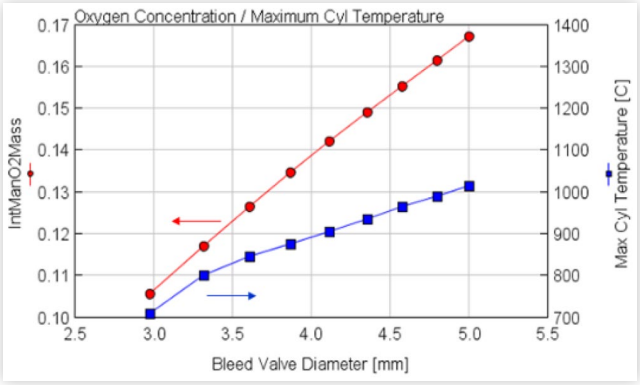

Increasing the oxygen content in the cylinder also resulted in an overall increase in the peak bulk in-cylinder gas temperature. This is seen in Figure 22. This observation is also related to the decrease in the combustion duration already discussed. As expected, the in-cylinder heat transfer rate shown in Figure 26 follows the shape of the peak in-cylinder bulk gas temperature.

A converse trend was shown in Figure 24 for the intake manifold temperature. It is shown that an increase in the bleed valve diameter resulted in a significant decrease of 25 °C. This can be interpreted as a result of a higher mass flow of cool fresh air supplied, which dilutes the hot recirculated gas.

Exhaust gas temperature experiences some "heating" due to re-compression during the exhaust stroke dependent on the volumetric flow rate passing through the exhaust valve. Furthermore, exhaust temperature was a composite of multiple mechanisms determined by interactions and "feedback" occurring in the shunt-pipe engine setup. One such mechanism "chain" can be described as follows: bleed valve diameter increases, oxygen content increases, faster burn, higher in-cylinder heat and a more effective expansion process (effective expansion ratio is larger) resulting in a *reduction* of exhaust temperature. Another "chain" with the opposite net result is: bleed valve diameter increases, oxygen content increases, faster burn, higher pressure increase due

FIGURE 23 The air supply mass flow rate and fluid power variation with a change in bleed valve restriction.

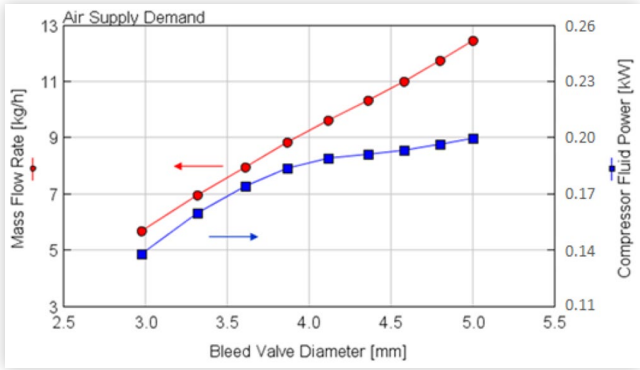

FIGURE 24 The intake manifold pressure and intake manifold gas temperature variation with a change in bleed valve restriction.

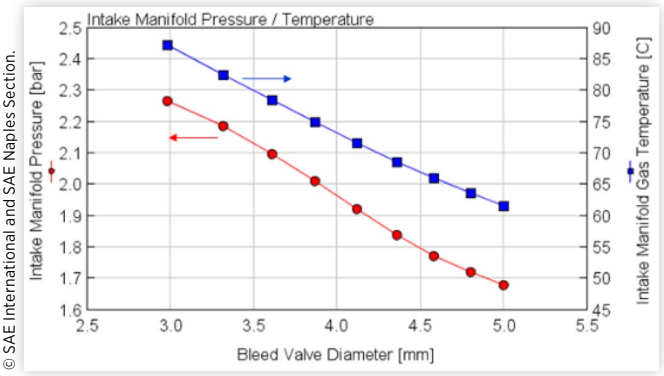

FIGURE 25 The burn duration and 50 % burn variation with a change in bleed valve restriction.

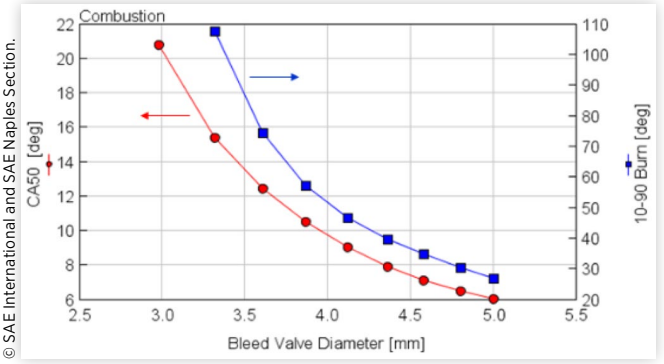

FIGURE 26 The heat transfer rate and exhaust manifold gas temperature variation with a change in bleed valve restriction.

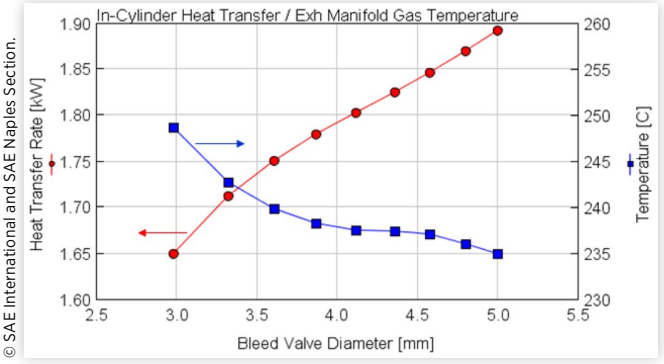

to combustion, reduced compression pressure needed to achieve desired PCP, reduced trapped mass by lowering of intake manifold pressure, reduced trapped mass gives a higher in-cylinder temperatures for a given fuel energy, resulting in an *increase* in exhaust temperature. Important to iterate that if the combustion process was assumed a constant profile, irrespective of composition and thermodynamic state, the results obtained from the model would be different. Hence,

the simulation was able to capture all these interactions due to the sub-models capturing gas-exchange, heat exchange and combustion effects.

Simulation Results - Part Three: Comparison between Conventional Pressurized Motoring, Fuelled Pressurized Motoring and Fired Engine Operation

The previous section dealt with the inner workings of the fuelled pressurized motoring method. The following section deals with a direct comparison between the conventional pressurized motored engine using air only, fuelled pressurized motoring (air + fuel), and the fully fired engine. The intention is that the reader can appreciate the trends and trade-offs along the progression from one method to the other. In the comparison being made, the simulation was set to produce the same peak in-cylinder pressure for all the three methods to ease comparison. The setpoint chosen for comparison was the 1400 rpm, 80 bar condition, for the same reason outlined in the previous section.

Figure 27 shows the in-cylinder pressure traces for the three methods. It is immediately noticeable how the conventional pressurized motored shows a significantly different shape than the fully fired engine, even though there is a match between the peak in-cylinder pressures. The differences in the rise and fall of pressure during compression and expansion, as well as the LPP are thought to induce a different FMEP "footprint" in the experimental engine, due to a different phasing between pressure and piston velocity. The fuelled pressurized motored case creates a balance between the two,

FIGURE 27 The crank angle resolved in-cylinder pressure for the conventional pressurized motoring, fuelled-motoring and fully fired.

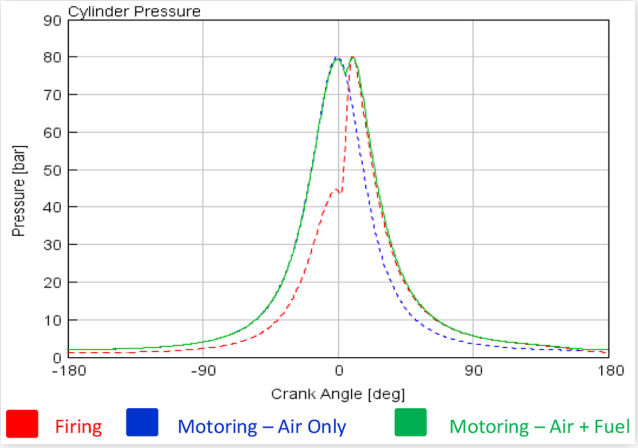

in the sense that it provides an LPP closer, or equal to that of the fully fired engine. It also provides similar loading on the expansion stroke. On the other hand the compression stroke seems to be more similar to that of the conventional pressurized motored engine. This trade-off happens because, the small heat released by combustion in the fuelled pressurized motoring is not able to give enough energy to raise the compression pressure by a very high quantity, hence the compression pressure should be made significantly high (by trapping a higher mass of gas) in order for the minimal combustion to just raise, and also shift the peak to the setpoint pressure.

Before proceeding with further comparisons and discussions, it should be made clear to the reader that whilst the graphs/properties for the conventional pressurized method are representative for the particular setpoint considered, they are not unique for the fuelled pressurized motored and the fully fired engine, due to their higher degree of freedom (e.g. injection quantity, injection phasing, bleed valve diameter for the fuelled pressurized motoring method, and the boosting system behavior of the fired engine). Hence the graphs and results being communicated in this section for the fuelled pressurized motoring and fully fired engines, are only intended to give an indication out of a very large number of possible combinations. The fired case was calibrated against dynamometer data at full load for the engine used in [5]. The selected case for the fuelled pressurized motoring was chosen such that the LPP was the parameter of focus. It should be appreciated that the experimenter/modeler might be more interested in obtaining a thermally fired-representative condition or a very high FMEP robustness factor rather than having a fired-representative LPP. This means that there is a trade-off to be made when shifting focus from one parameter over the other. Fortunately, the engine setup allows the flexibility to tailor to any particular focus (LPP, varying heat in the engine structure, or the highest FMEP robustness factor) while still achieving the desired PCP at a given engine speed.

Observing Figure 27, gives a better understanding how it is possible for the fuelled pressurized motored engine to give a late LPP, but still retain low IMEP and BMEP. Since the compression pressure for the fuelled pressurized motoring is relatively high compared to the fired engine, more work has to be expended in fuelled pressurized motoring, on the compression stroke. There is also less energy released since combustion is minimal. Due to this 'nearly symmetrical' pressure curve about TDC, the work done by the gas on expansion is very close in magnitude to the work done on the gas during compression. Consequently this results in a higher FMEP robustness factor, as shall be seen from a later figure (Figure 32). From the foregoing observation, it can be generalized that out of the very large testing spectrum allowed by the fuelled pressurized motoring method, condition B (i.e. double peak with virtually equal magnitudes) results in the highest FMEP robustness factor. It is noted that the very high FMEP robustness factor that can be achieved with the fuelled pressurized motoring results mainly from the flexibility of changing the IMEP, whilst still retaining it as a small value.

Figure 28 and Figure 29 show the brake and indicated mean effective pressures respectively. The brake and indicated mean effective pressures are negative for the conventional pressurized

FIGURE 28 The BMEP at different PCPs, for the conventional pressurized motored, fuelled-motored and fully fired.

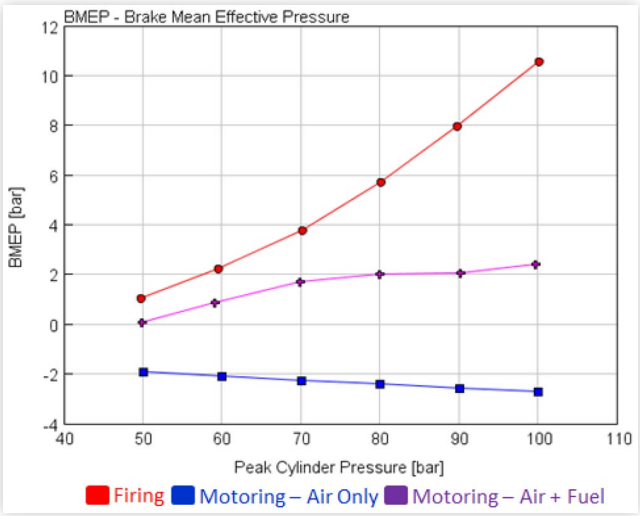

FIGURE 29 The IMEPnet at different PCPs, for the conventional pressurized motored, fuelled-motored and fully fired.

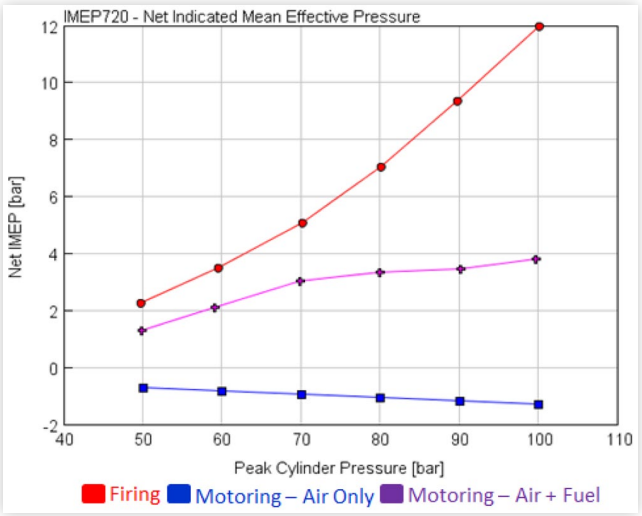

motored method, due to it requiring an external driver for supply of the engine losses. The fully fired engine has positive values which indicate power delivery from the engine. The fuelled pressurized motored method being plot in Figure 28 and Figure 29 show positive mean effective pressures, however it should be reminded that with this method, it is also possible to have negative and close to zero mean effective pressures. The curves for the fuelled pressurized motored in Figure 28 and Figure 29 are obtained at one particular injection combination.

The peak bulk in-cylinder gas temperature is shown in Figure 30. It is noticed that the conventional pressurized motored method displays a relatively constant temperature at all loading conditions. This was noted in [9], and also reported by Allmaier [6] and MAHLE [7]. The fuelled pressurized motored method also shows a relatively constant temperature

FIGURE 30 The peak bulk gas in-cylinder temperature at different PCPs, for the conventional pressurized motored, fuelled-motored and fully fired.

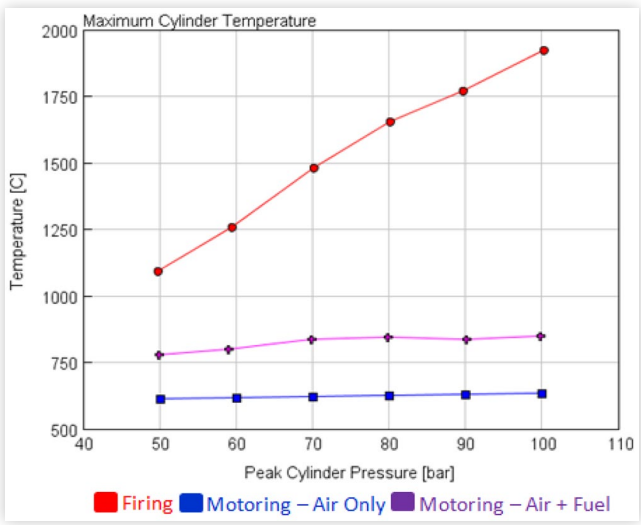

(at this chosen injection combination), but at a higher magnitude. This gives some advantage over the conventional pressurized motoring, as it approaches better the fired condition. It should be reiterated that according to the previous Figure 16, temperatures in the fuelled pressurized motoring can reach even higher magnitudes. The temperature shown in Figure 30, is for the injection conditions chosen for this comparative simulation run. It is interesting to see how the temperature in the fully fired engine spans a range of around 900 °C. This makes the evaluation of FMEP contributions from load and temperature difficult to obtain and understand. The conventional pressurized motoring, and to some extent, the fuelled pressurized motoring, both seem to decouple the effect of temperature from the effect of load. This allows an evaluation of the FMEP contribution from load and temperature separately, and controllably, depending on intake manifold pressure, temperature, gas composition (and for the fuelled pressurized motoring - injection conditions).

Figure 31 shows the average in-cylinder heat transfer rate as computed from the Woschni sub-model. It can be seen how the pressurized motored method displays a relatively low and constant heat transfer rate with PCP. This is attributed to the relatively low and constant in-cylinder temperature with PCP (and also engine speed). The fuelled pressurized motored engine shows a heat transfer rate which is higher than that for the conventional pressurized motoring, but lower than the pure firing. This is mainly driven by the in-cylinder temperature, which was relatively low for this chosen condition of operation of fuelled pressurized motoring. Higher values of heat transfer rate can be achieved if a different injection condition is selected to obtain higher in-cylinder temperatures.

Figure 32 shows the FMEP robustness factor for the firing, pressurized motoring using air only, and the fuelled pressurized motoring. It can be seen that at low in-cylinder peak pressures, all three methods give the highest robustness factor. This graph shows how the robustness factor is already increased significantly above that of the fired engine, with the

FIGURE 31 The average in-cylinder heat transfer rate at different PCPs, for the conventional pressurized motored, fuelled-motored and fully fired.

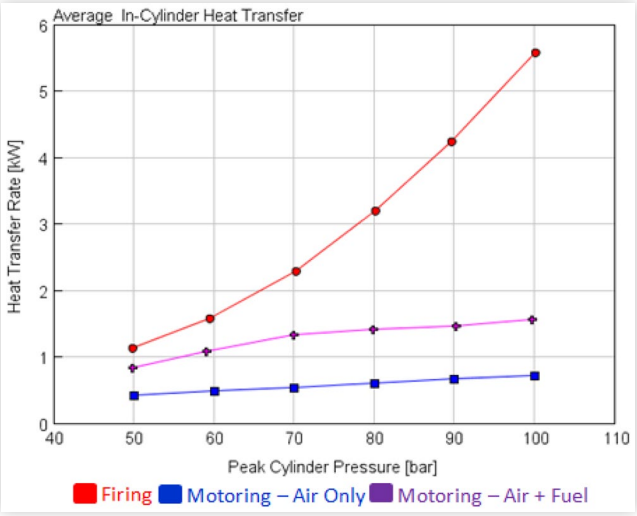

FIGURE 32 The FMEP robustness factor at different PCPs, for the conventional pressurized motored, fuelled-motored and fully fired.

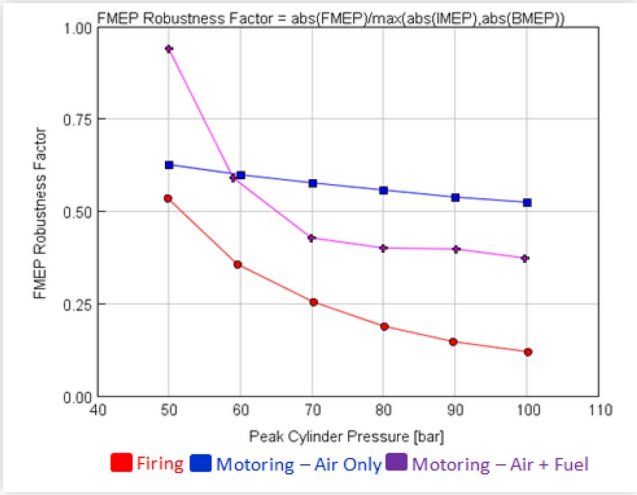

conventional pressurized motoring. The fuelled pressurized motoring case showed a range of FMEP robustness factors starting from a very high value of 0.9 (compared to 0.5 for the equivalent firing condition), to values of around 0.38 which fall between the other two methods.

The three sets of simulation results were presented and discussed in the previous sections. The first section presented simulation matrices for six different setpoints at fixed engine speeds, PCPs and bleed valve restriction. The injection duration and phasing were varied to achieve different LPPs, and consequently different FMEP robustness factors. The second set of simulation results was aimed at studying the effect of the bleed valve diameter. A particular setpoint was chosen and tested at fixed injection duration and phasing. The third set of simulation results consolidated the observations made with the previous results, as well as depicted a clearer image of the difference between the conventionally fired engine, the pressurized motoring using air, and fuelled pressurized motored engine. The next section discusses the salient results and observations presented in the previous sections.

Discussions

The simulation results have given a very positive outlook for this novel experimental method. The fuelled pressurized motoring method is the latest in a progression of proposed experimental test methods [5, 8, 9, 10] that give the experimenter:

1. Freedom to tailor the pressure history occurring in the cylinder, free from the constraints of the fired engine where peak cylinder pressure is intrinsically linked to engine torque/load, mostly dictated by the constraints of the combustion/ boosting system
2. A greatly enhanced FMEP robustness factor, meaning a reduction in the uncertainty of the FMEP measurement, at a very high degree of repeatability. These aspects would in turn benefit greatly the assessment of friction reduction technologies/ friction models

This freedom arises from the shunt-pipe / external supply system that ensures "boost-on-demand" (intake manifold pressure) at a very small air supply system resource, coupled with the addition of small amount of fuel to alter the LPP / mechanical loading behavior while adding important temperature/heat into the components to mimic the fired engine.

This flexibility was enabled by addition of fuel /combustion that has introduced new degrees of freedom that were not present in previous motored only methods. Given this added level of complexity it was felt that the simulation results be broken down into the three distinct parts.

The first part of the simulation results explored the role of injection timing and phasing for six different setpoint conditions of speed and peak in-cylinder pressure (PCP). A method was proposed for the simulation, but also for the experimenter, to eliminate two degrees of freedom by "locking" the air supply pressure to achieve the desired PCP (via a PID controller) and to keep the bleed valve constant for every speed/PCP setpoint. The influence of the injection quantity and injection phasing on relevant parameters such as peak in-cylinder pressure location, the IMEP, BMEP, PMEP and peak bulk gas in-cylinder temperature was shown. From these six simulation matrices it transpired that the fuelled pressurized motoring method is capable of producing a peak in-cylinder pressure which is close to that of fired engine operation. Apart from obtaining a similar peak in-cylinder pressure, it was also seen later, that fuelled pressurized motoring sustains an in-cylinder pressure over the expansion stroke similar to that in the fired engine. The extent to which the LPP is shifted depends mainly on the combination of the injection parameters chosen, together with the setpoint conditions of engine speed and peak in-cylinder pressure.

Apart from the 'theoretical' advantages that this method offers, it was found that it requires no expensive or complex apparatus. Practically, the method requires the apparatus that is usually already available in a fired engine, but with an

addition of a shunt pipe. It was also found that the fluid power required to pressurize the engine at the desired manifold pressure is manageable by a relatively small compressor.

Some interesting cases have emerged from the simulations, that are predicted to occur on the real engine. One such case is when the double-peak in-cylinder pressure was observed, with some cases having the later combustion peak smaller in magnitude than the compression peak. The reader should appreciate that even though this is not a condition at which a fully-fired engine would normally operate at, however at this condition, loading is still sustained over the expansion stroke. This means that even at this condition, the FMEP obtained from the equivalent experimental engine is able to provide information on the behavior of the FMEP at different phasing between instantaneous pressure (load) and piston velocity. Note that the "double equal peak" case - compression peak separate but equal in magnitude to the combustion peak - allowed to achieve a "late" LPP with a very low IMEP (more compression work) resulting in lower FMEP uncertainty.

Interesting cases around very low IMEP/BMEPs were observed, where the magnitude of FMEP even surpassed that of IMEP and BMEP. In the extreme case the IMEP and BMEP were of the same magnitude, meaning that FMEP was double that of either IMEP/BMEP (FMEP robustness factor = 2.0). It is hoped that the reader appreciates the significance of this high level of FMEP robustness (low uncertainty) while still achieving high cylinder pressures, up to the mechanical limit of the engine. A detailed engine friction model would greatly benefit from this type of experimental results.

Another interesting case is the zero BMEP case. For certain injection quantities (and to a lesser degree, injection phasing), the BMEP passed through the zero magnitude. i.e. engine neither requires motoring, nor provide mechanical power. Even though this condition was not deeply investigated, it might pose some practical advantages, if backed up by an appropriate control scheme. This creates a favorable condition both experimentally, but also economically. Some practical uses are the ageing of engines or friction stabilization without requiring very expensive dynamometer testbed, at a fraction of the fuel cost and still achieve any speed and any peak in-cylinder pressure. It should be re-iterated that retaining the engine at this condition without runaway, a strict fuel control scheme might be required. As stated earlier, this point was not investigated further and warrants further study.

From this first part of simulation results it was immediately apparent that the engine setup, consisting of a "shunt-pipe" recirculation, produces a high level of "feedback" where parameters change and in turn produce an intricate cascade of effects on other parameters. Simulation allowed insight on this feedback aspect, relieving the experimenter from the burden of understanding such behaviors given the more limited instrumentation available on the real engine.

The second part of the simulation results focused on the bleed valve restriction for a constant engine speed and peak in-cylinder pressure, and a constant injection quantity and phasing. It was shown that the direct effect of the bleed valve diameter (restriction) was the oxygen content in the system. Oxygen content affected the speed of combustion triggering a "cascade effect" on many parameters: contribution to the buildup of cylinder pressure due to combustion, the necessary compression pressure to sustain the desired peak cylinder pressure, the trapped mass in the cylinder and therefore the resulting in-cylinder bulk gas temperature and heat transfer given a fuel energy released, LPP. Increasing the bleed valve diameter also resulted in a higher fresh air supply flow rate, which meant a higher fluid power. It was however noted that even at maximum fluid power, the magnitude is still very small and manageable. Though the bleed valve produced complex behavior cascades, fortunately it could be set at a constant restriction for a given speed /PCP setpoint, granted enough oxygen is available at the highest injection quantity at the earliest phasing. This is the point where the simulation effort reaches its limit and the experiment intervenes, as the combustion aspect and, importantly, the effect on stability/ repeatability needs to be assessed on the real engine by observing the effect of varying of the bleed valve restriction. Confidence in combustion stability/ repeatability of the proposed experimental method was the short burn duration predicted by the combustion model, burn duration being a surrogate metric inferring COV.

To consolidate the study, the third and final part of the simulation results was a progression through the three different experimental methods: the pressurized motoring using air only, the proposed fuelled pressurized motoring, and the fully fired operation. These results allowed an evaluation of how the pressurized motoring methods fare against the fully fired engine. An evaluation was also made on the data quality and trade-offs.

The fired FMEP method (or fired indicating method) offers a very good representation of the real operating conditions on the FMEP measurement. It is however bound to very large uncertainty propagations due to the very low FMEP robustness factor induced by large IMEP uncertainties and to a lesser extent BMEP uncertainties. It also suffers from the COV induced by combustion (cycle-to-cycle variability).

The conventional pressurized motored using air only, on the other hand offers moderate FMEP robustness factors and very low COV. The shortcomings are the lack of the fired-like cylinder pressure to piston speed phasing given the peak pressure occurs always just before TDC, and the "cold" condition produced by achieving PCP with air compression alone. Using Argon as a working fluid [8, 9, 10], the pressurized motoring addressed this latter thermal aspect.

This simulation study predicts that this newly proposed fuelled pressurized motoring method is able to address the aforementioned shortcomings while leveraging the pressurized motored method to obtain even higher experimental data quality. The fuelled pressurized motoring allows a better representation of the fired condition on multiple accounts. Location of peak pressure can be moved after TDC, allowing for fired-type expansion stroke phased pressure to-piston speed profile and piston side forces. The burning of fuel introduces heat into the engine components / oil films closer to the real fired condition. Decoupling peak cylinder pressure from IMEP and BMEP provided the freedom of enhancing the FMEP magnitude over the IMEP/BMEP magnitudes, drastically reducing its measurement uncertainty.

Short of running the engine under normal fired conditions and accepting its high uncertainty in FMEP, the proposed pressurized fuelled motored method leverages its high flexibility, higher data quality and improved fired engine

fidelity to better characterize the fired condition. Its intrinsic simplicity and low resource requirement add to its attraction. What this new method cannot do is reproduce exactly the fired condition and improve FMEP experimental data quality at the same time in a single test. Some compromises have to be made and the method has its limitations.

In a single test of engine speed and PCP, the experimenter/analyst is required to make a compromise between;

- How closely matched is the pressure / crank angle history to the real fired case. This can be clearly seen in Figure 27, where the compression stroke deviates to some extent from that of the fired engine.
- The amount of heat /temperature in the cylinder. The injected fuel quantity is a fraction of the fired case, so heat/ temperatures have to be managed according to the intended focus of the study.
- Maximizing the FMEP robustness factor by reducing IMEP/BMEP for the same engine speed/PCP.

Strengths/discrepancies can be traded-off by choosing different combinations of injection strategy, air supply pressures and bleed valve restrictions. Multiple test variants can be conducted to leverage all the strengths to cover all aspects of the fired condition, simply not in one single test. It is felt that if a friction model is fed with all these test variants, at a higher experimental data quality, the confidence in such model is much higher than what is currently possible with the conventional fired FMEP, given its inherent uncertainty.

The limitation of the pressurized fuelled motored method is that at very high peak cylinder pressures, the relative contribution and hence flexibility introduced by the small quantities of fuel burnt diminishes. The advantages of the proposed method still apply over the competing methods at high PCP, albeit the narrower flexibility.

Conclusions

Shunt-pipe recirculation pressurized motoring experimental methods have shown their ability to reach fired-like cylinder pressures, high repeatability and higher FMEP data quality, while requiring low resources to conduct. Their limitations of fixed location of peak pressure around TDC have been addressed with this simulation study.

With the introduction of small quantities of fuel burnt inside the cylinder and a bleed valve to allow replenishment of oxygen to sustain combustion. Concerns of thermal runaway, instability or oxygen starvation for combustion were predicted to not occur in the engine. A control method to achieve this was suggested.

The main goal of the study, to achieving a wide range of LPP for a given fixed peak in-cylinder pressure and fixed engine speed, was reached. The fuel burnt had the added benefit of raising gas temperatures and in-cylinder heat transfer rate closer to the fired condition. This allows a better representation of the FMEP contribution from thermal expansions and oil film viscosities changes.

The added degrees of freedom by introduction of the fuel resulted in essentially a decoupling of IMEP from peak cylinder pressure. Having independent control of IMEP meant that IMEP/BMEP magnitudes could be brought down to FMEP magnitudes, effectively reducing experimental FMEP uncertainty by reducing uncertainty propagation, all of this at the same desired peak cylinder pressure of the fired engine

The idealized experimental test would be the real engine's fired case which does not suffer from the FMEP measurement uncertainty inherent in conventional "Fired FMEP method". The proposed fuelled pressurized motoring method moves closer to this ideal because of its broad flexibility of reaching the same peak cylinder pressure in a multitude of ways, while generating FMEP data with a much lower uncertainty. Having a robust method which allows the experimental engine to be tested over a wide spectrum of conditions can provide benchmark results against which the FMEP models can be tested and validated. These models can in turn be adapted to unexplored engine architectures for which experimental data is not available yet.

Suggestions for Further Studies

The simulation study seems to present no major setbacks for the experimentalist; however it is appreciated that some practical endeavors, especially when dealing with the control strategy of the engine might be more challenging than they appear. As a result, the next step in developing further this method requires the implementation on the experimental engine.

In this work, a CI engine with diesel fuel injection was considered. It is unknown how a SI engine with petrol fuel behaves with this presented method. It is thought that the lower COV for CI engines can present an advantage over the application of the method with the higher COV SI engines.

The bleed valve was retained constant throughout the simulation matrices conducted. It might present additional advantages to the method if the bleed valve diameter is PID-controlled and allowed to vary accordingly for the same test conditions of engine speed and peak in-cylinder pressure. Even though this suggestion might provide advantages to the method, it is expected to add some higher degree of complication as regards to apparatus and control requirements on the experimental engine.

The condition of zero BMEP which was explained in a previous section is one which requires some additional investigation. It is thought that further development to this observation might present advantages in stabilizing of engine friction and ageing of engines.

References

1. Mufti, R.A., and Priest, M., "Experimental Evaluation of Piston-Assembly Friction under Motored and Fired Conditions in a Gasoline Engine," *Transactions of the ASME* 127:826-836, Oct. 2005.
2. Pranay, N., and Scott, M., "Friction between Piston and Cylinder of an IC Engine: A Review," SAE Technical Paper 2011-01-1405, 2011, https://doi.org/10.4271/2011-01-1405.

3. Mauke, D., Dolt, R., Stadler, J., Huttinger, K. et al., *Methods of Measuring Friction under Motored Conditions with External Charging* (Switzerland: Kistler Group, 2016).
4. Richardson, D.E., "Review of Power Cylinder Friction for Diesel Engines," *Transactions of the ASME* 122, 2000.
5. Caruana, C., Farrugia, M., and Sammut, G., "The Determination of Motored Engine Friction by Use of Pressurized 'Shunt' Pipe between Exhaust and Intake Manifolds," SAE Technical Paper 2018-01-0121, 2018, https://doi.org/10.4271/2018-01-0121.
6. Allmaier, H. et al., "An Experimental Study of the Load and Heat Influence from Combustion on Engine Friction," *International Journal of Engine Research* 17(3):347-353, Mar. 2015.
7. MAHLE International GmbH, "Engine Testing," *Pistons and Engine Testing* (Stuttgart, Germany: Springer), ch. 7, 117-281.
8. Caruana, C., Farrugia, M., Sammut, G., and Pipitone, E., "Further Experimental Investigation of Motored Engine Friction Using Shunt Pipe Method," *SAE Int. J. Adv. & Curr. Prac. in Mobility* 1(4):1444-1453, 2019, https://doi.org/10.4271/2019-01-0930.
9. Caruana, C., Pipitone, E., Farrugia, M., and Sammut, G., "Experimental Investigation on the Use of Argon to Improve FMEP Determination Through Motoring Method," SAE Technical Paper 2019-24-0141, 2019, https://doi.org/10.4271/2019-24-0141.
10. Caruana, C., Farrugia, M., Sammut, G., and Pipitone, E., "Further Experiments on the Effect of Bulk In-Cylinder Temperature in the Pressurized Motoring Setup Using Argon Mixtures," SAE Technical Paper 2020-01-1063, https://doi.org/10.4271/2020-01-1063.
11. Pipitone, E., Beccari, A., and Beccari, S., "The Experimental Validation of a New Thermodynamic Method for TDC Determination," SAE Technical Paper 2007-24-0052, 2007, https://doi.org/10.4271/2007-24-0052.
12. Woschni, G., "A Universally Applicable Equation for the Instantaneous Heat Transfer Coefficient in the Internal Combustion Engine," SAE Technical Paper 670931, 1967, https://doi.org/10.4271/670931.
13. Finol, C.A., and Robinson, K., "Thermal Modelling of Modern Engines: A Review of Empirical Correlations to Estimate the In-Cylinder Heat Transfer Coefficient," *Proceedings of the Institution of Mechanical Engineers, Part D: Journal of Automobile Engineering* 220(12):1765-1781, Dec. 2006.
14. Chen, S., and Flynn, P., "Development of a Single Cylinder Compression Ignition Research Engine," SAE Technical Paper 650733, 1965, https://doi.org/10.4271/650733.
15. Livengood, J.C., Rogowski, A.R., and Taylor, C.F., "The Volumetric Efficiency of Four-Stroke Engines," *SAE Quarterly Transactions* 6(4):617-636, Oct. 1952.
16. Heywood, J.B., "Gas Exchange Processes," *Internal Combustion Engines Fundamentals* (McGraw-Hill Series in Mechanical Engineering, 1988), 211.

Contact Information

Gilbert Sammut
Jaguar and Land Rover
gsammut@jaguarlandrover.com

Mario Farrugia.
Mechanical Engineering Department,
University of Malta, Malta.
mario.a.farrugia@um.edu.mt

Acknowledgments

The research work disclosed in this publication is partially funded by the Endeavour Scholarship Scheme (Malta). Scholarships are part-financed by the European Union-European Social Fund (ESF)-Operational Programme II-Cohesion Policy 2014-2020 "Investing in human capital to create more opportunities and promote the well-being of society".

Definitions/Abbreviations

ATDC - After Top Dead Centre
BBDC - Before Bottom Dead Centre
BDC - Bottom Dead Centre
BMEP - Brake Mean Effective Pressure
BTDC - Before Top Dead Centre
CAD - Crank Angle Degrees
CI - Compression Ignition
COV - Coefficient of Variation
ECU - Engine Control Unit
EVO - Exhaust Valve Opened
FMEP - Friction Mean Effective Pressure
HDi - High-Pressure Direct Injection
IMEP - Indicated Mean Effective Pressure
IVC - Intake Valve Closed
LPP - Location of Peak In-Cylinder Pressure
MAP - Manifold Absolute Pressure
OEM - Original Equipment Manufacturer
PCP - Magnitude of Peak In-Cylinder Pressure
PID - Proportional - Integral - Derivative
PMEP - Pumping Mean Effective Pressure
SI - Spark Ignition
SOI - Start of Injection
TDC - Top Dead Centre

e-ISSN 2641-9645